Results in Engineering 28 (2025) 107890

Contents lists available at ScienceDirect

Results in Engineering

journal homepage: www.sciencedirect.com/journal/results-in-engineering

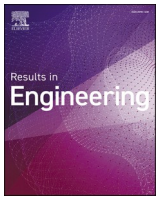

Soiling of solar-field heliostats during operation in concentrating solar thermal plants

Johannes Wette [a,*], Florian Sutter [b], Raúl Enrique-Orts [a], Manuel Pérez-García [c], Ricardo Sánchez-Moreno [a], Aránzazu Fernández-García [a]

[a] Centro de Investigaciones Energéticas, Medioambientales y Tecnológicas (CIEMAT). Plataforma Solar de, Almería (PSA), Ctra. de Senés s/n km 4, Apartado 22, 04200, Tabernas, Spain
[b] German Aerospace Center (DLR), Institute of Solar Research, Calle Doctor Carracido 44, 1st floor, 04005 Almería, Spain
[c] University of Almería-CIESOL Carretera Sacramento s/n, 04120 La Cañada de San Urbano, Almería, Spain

ARTICLE INFO

Keywords:
Concentrated solar thermal
Heliostat
Stow position
Solar reflector
Soiling
Reflectance

ABSTRACT

Solar energy conversion is highly affected by soiling of collector surfaces, potentially decreasing the yield of running systems. Design, operation, and maintenance strategies of solar energy plants have the potential to mitigate the most severe consequences of soiling. In this study, the soiling of tracked heliostats of concentrating solar thermal technologies based on central receiver systems is investigated and how the selection of the stow position during inactivity impacts the soiling of the reflectors used. For this, a long duration campaign was conducted, covering more than a whole year at a central tower system of the CIEMAT-Plataforma Solar de Almería, with regular measurements on two heliostats during realistic operation. Two stow positions were chosen to compare between the heliostats: the reflector side facing-up towards the sky and down towards the ground. Important benefits in soiling protection were detected for the face-down option, resulting in a nearly seven times lower soiling rate for this case compared to the face-up position. This results in a higher yearly average cleanliness of 0.984 for face-down compared to 0.895 for face-up stow. Further key parameters were investigated, such as tracking-stow time ratio, inclination and height above ground, and the used measurement equipment, and their impact on soiling was quantified. The results of this study are intended to serve as an input parameter for future developments, concerning new heliostat designs, operational strategies and measurement procedures.

1. Introduction

Climate change has been identified as one of the key challenges humanity is facing in the present by the global community and recognized by international institutions as the United Nations and the World Economic Forum [1,2]. Renewable energies play a crucial role in the necessary decarbonization of human activities by decreasing the reliance on fossil fuels and the emission of greenhouse gases [3]. One of the main sources of renewables is solar energy, which has seen a tremendous growth over recent years due to its advances in efficiency and its substantial cost reductions [4]. This growth was mainly driven by photovoltaics (PV), but to a lower extent also by concentrated solar thermal (CST) technologies [5]. The potential for CST and its importance for the future development is mainly seen in its ability to provide efficient energy storage for extended periods of time and the direct delivery of process heat at different temperature ranges [6].

To assure the growth and commercial success of solar energy technologies, efficiencies and costs have to further decrease. Operation and maintenance (O&M) of commercial plants plays an important role here [7]. One factor that can negatively influence the efficiency of the plants and have an impact on O&M, is the soiling of the solar collectors (PV panels and CST reflectors). The effect of soiling is direct by lowering the optical efficiency of the system, decreasing the converted energy, and indirect by increasing the need for the cleaning of the collectors, leading to higher expenses in O&M (labor, energy, water, etc.) [8,9]. A study from 2019 estimated the global annual revenue losses due to soiling for solar energy applications to 4–7 billion € in 2023 [10]. Favorable solar resources (high annual solar irradiation) frequently exist at locations, where at the same time the climate is arid and potentially desertic [11–13]. These places are often characterized by high loads of airborne dust and sand. These kinds of particles can precipitate on the solar

* Corresponding author.
E-mail address: johannes.wette@psa.es (J. Wette).

https://doi.org/10.1016/j.rineng.2025.107890
Received 30 April 2025; Received in revised form 16 October 2025; Accepted 21 October 2025
Available online 22 October 2025

Nomenclature

Symbols

θ_i	Incidence angle [°]
λ	Wavelength [nm]
ρ	Reflectance [-]
$\rho_{s,\varphi}$	Solar-weighted near-normal near-specular reflectance [-]
$\rho_{\lambda,\varphi}$	Spectral near-normal near-specular reflectance [-]
ρ_{clean}	Reflectance in clean state [-]
ρ_{soiled}	Reflectance in soiled state [-]
φ	Acceptance (half) angle [mrad]
SR	Soiling rate [%/day]
ξ	Cleanliness [-]
$\overline{\xi}$	Mean cleanliness [-]
r_t	Tracking to stow ratio [-]
c_{P10}	Average particle concentration < 10 μm in diameter [10,000 particles 1/l]
r_{sum}	Daily precipitation sum [mm]
v_{max}	Maximum daily wind speed [m/s]

Acronyms

CIEMAT	*Centro de Investigaciones Energéticas, Medioambientales y Tecnológicas*
CRS	Central receiver system
CST	Concentrating solar thermal
D&S	Devices & Services
O&M	Operation and maintenance
PSA	Plataforma Solar de Almería
PTC	Parabolic trough collector
PV	Photovoltaic
S2R	Spectral Specular Reflectometer

collector surfaces and harm their optical efficiency in a severe manner [14].

All CST systems use this kind of optical surfaces to concentrate solar irradiation. The concentration is achieved by redirecting the incoming solar irradiation on a large collector area to a much smaller receiver area. Almost exclusively, this concentration is achieved through the use of mirrors, also called reflectors [15]. Only in very rare cases with alternative designs, lenses are used instead [16,17]. The mirrors reflect the incoming solar irradiation and focus it on a receiver point or line, depending on the technology. In the case of parabolic-trough collectors (PTC) single-axis tracked curved mirrors focus on a receiver tube. In the case of central receiver systems (CRS) a large amount of heliostats, each comprised of various reflector facets, are dual-axis tracked to focus onto the receiver of a central tower. Only direct irradiation can be used for the concentration, which means that any diffuse part, for example on cloudy or hazy days, is lost for the energy conversion process. In the same way, irradiation that is scattered on the reflector surface cannot be concentrated onto the receiver [18]. This is also the reason why soiling plays a much stronger role for CST systems than for PV ones: on PV panels, scattered light can still be converted as long as it is not scattered away from the panel surface or absorbed by the soiling particles [10]. Due to this higher effect of soiling phenomena in CST systems, the here presented work is strictly focused on CST concentrators.

The main parameter for the evaluation of reflectors used in CST systems is the reflectance, ρ. It determines the ratio of the incoming energy that can be reflected onto the receiver [19]. It is also used to determine the influence of soiling on the reflector's optical efficiency. To this end, usually the cleanliness of the reflector, ξ, is calculated by dividing the ρ in the soiled state by the initial value in the perfectly clean state [20]. The reflectance is a complex parameter depending on various important variables, such as the wavelength, λ, and incidence angle, θ_i, of the incoming light rays and the acceptance angle, φ, which determines the amount of scattering included away from the perfectly specular direction of reflection. These parameters are highly technology and site specific. To account for the influence of these different parameters, the most significant value for a solar reflector is the solar-weighted near-specular reflectance, $\rho_{s,\varphi}$ [21]. For this, ρ is weighted over the whole solar spectrum at θ_i and φ representative of the specific case (e.g. technology, site, plant geometry). Weighting is usually done in a range of λ=[320, 2500] nm (named as solar range). Measurements are mainly performed at near-normal θ_i (usually below 20°), even though higher angles are common in real applications and might be investigated. The most typical φ used for measurement is 12.5 mrad as it is representative for commercial PTC plants and within the realistic range for CRS plants [22,23]. Much lower φ occur especially in tower plants and it may be necessary to take them into account as well.

The most common approach to measure reflectance and cleanliness directly in the solar field is by the use of handheld portable reflectometers. A series of commercial devices are on the market and all have limitations regarding the measured parameters [24,25]. That means that they don't measure in the whole wavelength range, usually only at one or few discrete wavelengths, and they are limited to certain acceptance angles and a fixed near-normal incidence angle. The most commonly used equipment are the D&S-15R by Devices & Services, Condor by Zepren, pFlex by PSE, CM700d by Konica Minolta and a series of gloss meters designed for the measurement of gloss of paints and coatings (e.g. ZGM-1130 by Zehntner). Alternative techniques are also used, such as stationary autonomous sensors (TraCS, AVUS, dustIQ, etc.), which usually do not measure the reflector facets themselves but rather extra samples exposed in the solar fields [26–28]. In recent years, investigation is performed on the use of image based techniques, which allow for the measurement of larger reflector areas, usually with a trade-off in accuracy [29–31]. Knowledge of the actual state of reflectance of the solar field reflectors is important because it serves as an input parameter for the O&M of the plant. It is used for the scheduling of cleaning tasks and for yield calculations among others [32,33]. For a more accurate determination of reflectance parameters, laboratory measurements can be performed. Spectrophotometers are used to measure the spectral hemispherical reflectance in the relevant solar range to detect changes depending on the wavelength. A few specialized prototype devices exist with the capability of determining the more relevant solar-weighted near-specular reflectance [34].

The investigation of soiling of solar reflectors has received increased interest over recent years, especially with the ongoing construction of commercial power plants at locations where increased soiling development is expected, such as the Middle aEst and North Africa, in places adjacent to or in deserts [35,36]. The research focuses on topics such as parameters influencing the soiling, the mitigation of soiling deposition, and the measurement procedures to determine the magnitude of its influence.

A variety of soiling rates, *SR*, of considerably different magnitudes from different sites can be found in the literature. It has to be taken into consideration that these soiling rates have been determined using different measurement equipment, thus evaluating different reflectance parameters, and varying exposure conditions, such as used reflector material, inclination and position of reflectors, tracking versus static positioning, measurement frequency and duration of exposure campaigns. The soiling rate is usually expressed as daily cleanliness loss as %/day. Mean values of *SR* over extended periods of time, often several months, reported in the literature comprise values from tenths of a percent per day up to several percent [32,37–40].

Several studies looked at the influence of the inclination of the

reflector surfaces on the soiling behavior [35,41,42]. All CST systems use tracked concentrators to account for the changing position of the sun throughout the day and the year and to always focus the direct solar radiation on the fixed focal point or line. In addition, the concentrators are usually put in a stow position when inactive, e.g. during the night, maintenance procedures or for safety reasons and high wind situations. The consensus in the community is that lower inclination surfaces facing up (near horizontal) are affected more severely by soiling than higher inclinations (closer to the vertical position) or down-facing surfaces. The main reasons behind this behavior are the gravity induced downward settling of airborne dust particles and reduced particle removal by changing water/humidity induced processes [43–46].

There is a variety of different heliostat designs that are being used for the solar fields in CRS, which differ quite considerably from each other. An overview of existing commercial designs and those under development is presented in [47]. The first striking difference is in the size of the single heliostats. Designs vary from around 1 m^2 of reflective area to over 120 m^2 per heliostat. There is no clear consensus on the optimal size, which may depend on factors such as field and tower size, concentration ratio, and site location, among others. The designs also differ in the drives used to facilitate tracking of the heliostat, material and geometry of the used reflector facets and control system. A particular feature of some of the designs is their ability to position the heliostat with the front reflective side facing downwards, and with that stowing the heliostat in a horizontal position facing the ground. Necessary specifications for this face-down option include drives with sufficient flexibility and usually a vertical gap in the reflector surface where the vertical heliostat pedestal is located [48]. Studies were conducted in the early development phase of CST systems at the end of the 1970′s in the USA, investigating the effect of stow position on the soiling behavior (and other parameters) and evaluating its economic viability, comparing costs of soiling mitigation and additional manufacturing costs [49]. Data for soiling rates were obtained from small samples and several heliostats over various months. Substantial variations were detected for soiling rates depending on the positioning of the surfaces. In [50,51] economic analysis was performed based on this data and concluded that vertical stow may be the most cost effective strategy. It was pointed out that vertical stow may not be feasible in all systems and that the ability to face-down stow could lead to overall cost savings depending on site conditions and specific heliostat design choices. During these studies, relatively low soiling rates of maximum ca. 0.45 %/day were found even for face-up stow. Another point to bear in mind is the complexity to compare these results to nowadays studies for several reasons: experimental reflectance measurement techniques were used, data from samples and heliostats of different reflector materials were joined (glass, acrylic, etc.), and evaluations were then used for a specific design in question, etc.

Recently, a roadmap was published by the international Heliocon consortium [52], led by the National Renewable Energy Laboratory, NREL, from the USA and comprising various research institutions and industry stakeholders to foster advances in heliostat development [53]. This roadmap identifies the most pressing tasks to be addressed for the future commercial deployment of the technology in the near future to decrease costs and increase efficiency. A specific subtask in the roadmap is dedicated to the topic of soiling, addressing impacts and mitigation techniques. It is highlighted that O&M is a major cost driver and the influence of soiling on O&M is significant. It is recommended to address topics such as the creation of a soiling database for characteristic sites, and the understanding of trade-offs between soiling due to operation strategies and factors such as design choices. It is specifically stated that there is a lack of understanding of the influence of the stow position on the soiling behavior of heliostats and the implications this has.

The study presented in this article addresses several of the above-mentioned open points, with the main objective of analyzing the impact of different stow positions on the soiling of heliostat reflectors. A long term measurement campaign was conducted, consisting of state-of-the-art reflectance measurements to determine soiling on solar tower heliostats, covering more than a whole year in an experimental heliostat field at the CIEMAT-Plataforma Solar de Almería (PSA). The investigated heliostats are in tracking over the entire campaign duration with different night time stow positions, including face-up and face-down stow, and this represents conditions very similar to the ones observed in commercial plants. This provides data with a duration and regular frequency not previously reached in other studies, especially for operational heliostats. In addition, the influence of further factors is investigated, such as daily tracking time and the height above ground of the facets on the soiling behavior, the impact of further surface inclinations and the influence of the used measurement equipment on the significance of the reached results. The study is limited to the impact on soiling, but no further economic analysis is performed, concerning the viability of implementing face-down stow capabilities of potential heliostat designs or the adaptation of O&M strategies. The here presented findings on soiling rates are intended to serve as input parameters for future studies in these directions, as the involved parameters, e.g. specific design choices and local climatic parameters, are highly case sensitive. Even though the absolute numbers may change at different sites, the findings can be used by stakeholders, mainly by developers to decide on the implementation of a face-down stow capability in novel heliostat designs and for operators to adapt their O&M strategies, to reduce cleaning effort through an improved stowing strategy.

2. Methodology

In this section, the methodology for the conducted study is presented. Firstly, the PSA with its CESA1-heliostat field, where the two selected heliostats are located, is introduced. Secondly, the devices used for the measurements are described and the parameters of the evaluated campaigns are explained in detail. Finally, the description of the three experimental campaigns is included: 1. The main campaign comprised regular reflectance measurements, with portable reflectometers on the two heliostats in tracking throughout a whole year, with cleaning after all measurements. 2. A shorter, several months long, extra campaign was also performed with a higher daily tracking time. 3. Finally, additional measurements were performed during the small sample campaign in the laboratory on reflectors samples of around 10 × 10 cm^2, previously installed at the same site as the heliostats.

2.1. Heliostat field description

The PSA provides installations including all major technology types used in CST applications. Among others, it has several CRS with the corresponding heliostat fields. The main CRS is the CESA-1 tower, with a field of 300 dual-axis tracking heliostats of approximately 40 m^2 of reflective area each. Fig. 1 displays the two selected heliostats for this campaign on the left and an aerial view of the whole field layout on the right. It is located in southern Spain at 37°06′ North, 2°21′ West with a semi-arid climate. As the PSA is a research facility, its main goal is not maximizing operation time as in commercial CST plants. Meteorological data is collected continuously at site. The main parameters with a potential impact on soiling are presented in the results section alongside the campaign data. The presented parameters are the accumulated daily precipitation, r_{sum} [mm], the maximum daily wind speed, v_{max} [m/s], and the average particle concentration below 10 μm in diameter, c_{P10} [in 10,000 particles 1/l]. Operation times depend on specific running projects and the normal operation mode for heliostats, when they are not focused on a receiver is off-focus tracking. This mode consists of tracking and focusing the heliostats on one or several points in the air close to the tower, quasi stand-by mode, to accumulate operation time of the components (drives, sensors, etc.) and to avoid damage of components due to inactivity.

The heliostat design allows the movement of the elevation axis in a range of approximately 180° between the two extreme horizontal

Fig. 1. The two heliostats, H18 and H20, used for the campaign during tracking (left) and the layout of the CESA1 solar field with position of heliostats (right).

positions, with the reflector front side facing the sky (face-up) and facing the ground (face-down). For the ability to move in the face-down position, a vertical gap between mirror facets in the center of the heliostat, where the pedestal is located with a width of 90 cm is left free, which reduces the potential reflective area of the heliostat. In Fig. 2, both heliostats can be seen in their respective stow positions, in the background the one facing down and in the foreground facing up.

The material used as the reflector of the heliostats is a commercial 4 mm silvered-glass mirror. This represents the most common, commercially used type of mirror. Each mirror facet measures approximately 149×110 cm^2. Per heliostat, four facets make up one horizontal row, with six rows vertically, totaling 24 facets per heliostat.

For this study, two heliostats, labeled H18 and H20, were chosen that are in a position directly adjacent to each other, to assure same exposure conditions, such as wind, dust, etc. The heliostat's location is at the eastern edge of the solar field and this way facing one of the main wind directions at the PSA site, with the wind coming mainly from the east.

2.2. Measurement devices

The main device used for the reflectance measurements in the solar field is the D&S-15R reflectometer developed by Devices & Services (D&S, Fig. 3a). Monochromatic near-specular reflectance, $\rho_{\lambda,\varphi}$, measurements are performed at φ=12.5 mrad acceptance angle and the illumination is provided by a red LED source with a spectral peak at λ=660 nm at θ_i=15° The device allows to change φ depending on the specific task. For this study, the 12.5 mrad were chosen, because it is the most commonly used angle and it is representative for PTC and CRS technologies, as explained in the introduction. Due to the small φ of the device, manual alignment has to be performed when placing it on the

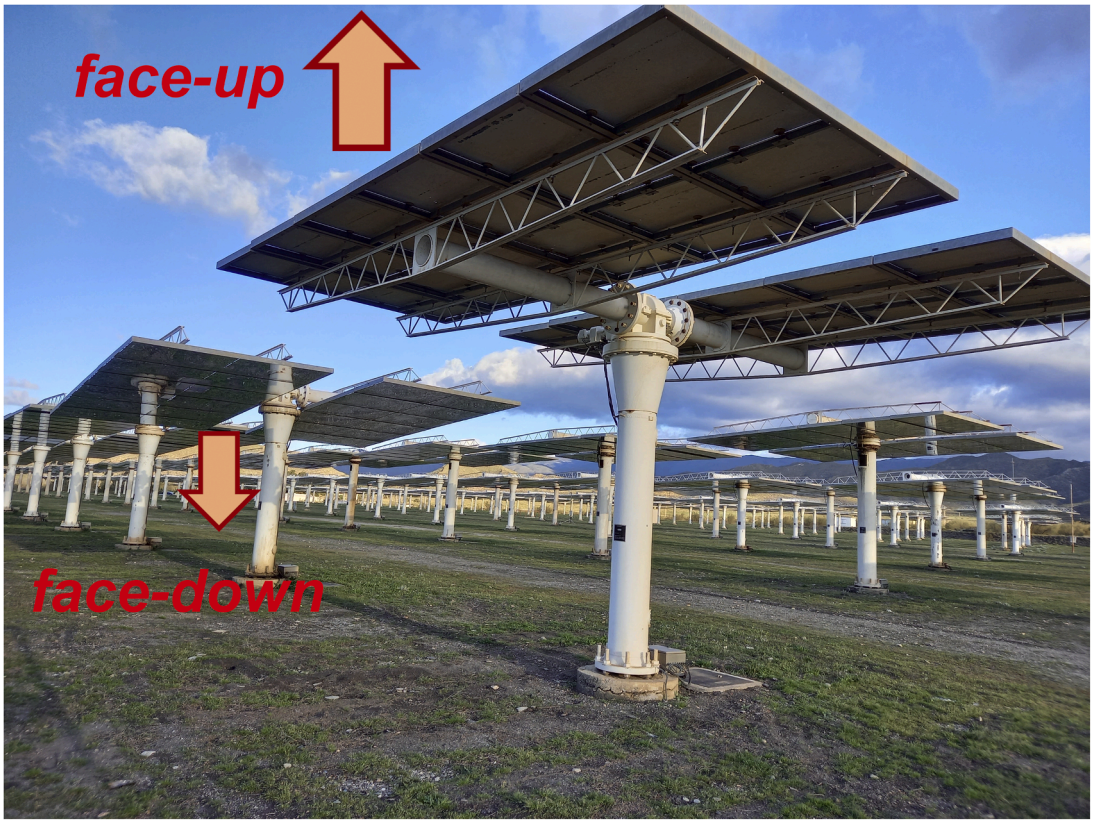

Fig. 2. The two campaign heliostats in stow position, reflector front side marked with red arrows. Face-down heliostat H18 in the background and face-up heliostat H20 in the foreground in the image.

Fig. 3. Reflectometer devices used for field measurements, a) D&S-15R on the left and b) Condor by Zepren on the right.

reflector surface, to assure the interception of the reflected light by the internal aperture and sensor.

Additional measurements were performed with the Condor reflectometer manufactured by Zepren (Fig. 3b). This device uses a higher acceptance angle compared to the D&S-15R of φ=145 mrad. The much higher φ admits measurements without prior manual alignment and therefore a considerably easier handling, including more scattered light in the measurement. The Condor measures at θ_i=12° in six discrete λ = {435, 525, 650, 780, 940, 1050} nm, and provides the solar-weighted reflectance value based on these. The value at λ = 650 nm is used for the direct comparison to the D&S-15R value at similar wavelength. The Condor was chosen as an alternative reflectometer to analyze the influence of the use of different measurement equipment on the results. Due to its easy handling and high reliability, the Condor is one of the standard alternative equipment used in numerous commercial plants. It possesses the highest acceptance angle among the commercial types and thus important differences are expected [25].

To determine the solar-weighted near-specular reflectance, $\rho_{s,\varphi}$, of the small reflector samples in the laboratory, the Spectral Specular Reflectometer (S2R) is used. This is a laboratory reflectometer, designed as an accessory for the commercial Lambda 1050 spectrophotometer by Perkin Elmer, based on the General Purpose Optical Bench (PELA1003) [54]. With the S2R it is possible to determine the spectral near-specular reflectance, $\rho_{\lambda,\varphi}$, in the solar range from 320 to 2500 nm, with θ_i ranging from near normal (ca. 10°) to close to 90° and φ between 7.4 and 107.4 mrad. With the spectral reflectance, the determination of the solar-weighted reflectance is possible, by the weighting with the solar irradiance standard spectrum IEC 60,904 [55]. For this campaign, measurements were performed at θ_i={15, 30}° and φ=12.5 mrad. The 15° incidence angle was chosen because it represents near-normal conditions, similar to the portable devices, and the 30° was added because it represents a more realistic mean value, appearing in the heliostat field over the course of a whole year for the PSA case [22]. The solar-weighted value at 30° is used in the end as the reference value, the reflectometer values are compared to, because it is the most significant one determining the optical quality of the reflectors at this site.

2.3. Field measurement procedure

The main measurements performed during the study, are reflectance measurements taken with the D&S-15R reflectometer. The reflectance measurements are used to determine the cleanliness of various facets of the selected heliostats, by comparing the actual reflectance value to the one in the clean state. Two facets per heliostat were selected from the lowest line of facets on the heliostat area, because this line provides the easiest access from the ground. The facets are identified by the heliostat number and facet ID (H18–1, H18–3, H20–1, H20–3), as indicated in Fig. 4 left. To analyze the influence of the height of the facets on the soiling, during the extra campaign, two additional facets on the fifth line counted from the bottom were measured and compared to the first line (see Fig. 4 left), named H18–51, H18–53, H20–51, H20–53. The height above ground of facets changes with different tracking positions. The facets of the lowest line are approximately 1 m above the ground when the heliostat is positioned vertically compared to around 6 m for the fifth line. All facets are at roughly 3.5 m above ground in horizontal position.

On every facet, a total of 30 measurements are taken, with the dimension of the facets and the distribution of the measurement spots shown in Fig. 4 right. 20 measurements are evenly distributed over the whole surface to determine the mean reflectance and thus cleanliness of the facet (red circles in the image). 10 additional measurements are taken on a line on the lower edge, approximately 10 cm from the facet edge (blue circles in the image), because from previous observation it was known that patterns of heavier soiling develop on these lower edges. The 10 additional measurements are treated separately from the 20 main ones in the results section. The 20 measurements per facet are already a higher number than the usually performed ones and cited in literature, to be sure to achieve statistically relevant results [25,56]. All measurements are taken without a measurement mask or similar, but placing the reflectometer, the D&S or Condor, by hand. This way, the exact positions of the single measurements change slightly from one measurement to the other without a strong influence on the facet mean values. To confirm the significance of this method with 20 measurements, before the campaign start this process was repeated four times on two separate facets. Values from these four measurement series are compared to check the deviation between the measurement series and if there is even a trend in the change, due to a potential influence of the measurement process, by touching of the soiled surface by the reflectometer.

As explained in the introduction, the main parameter to evaluate soiling of solar reflectors is the cleanliness ξ. It relates the actual state of reflectance at any point in time to the initial reflectance in the perfectly clean state, as indicated in Eq. (1). A value of 1 represents a perfectly clean mirror and values between 0 and 1 correspond to different levels of soiling. The lower the value, the more intense the soiling is. This parameter is independent of the initial cleanliness and this way it is possible to compare the soiling of materials with different initial reflectance values. Cleanliness values may differ depending on the used reflectance parameters, such incidence angle, acceptance angle, etc. The

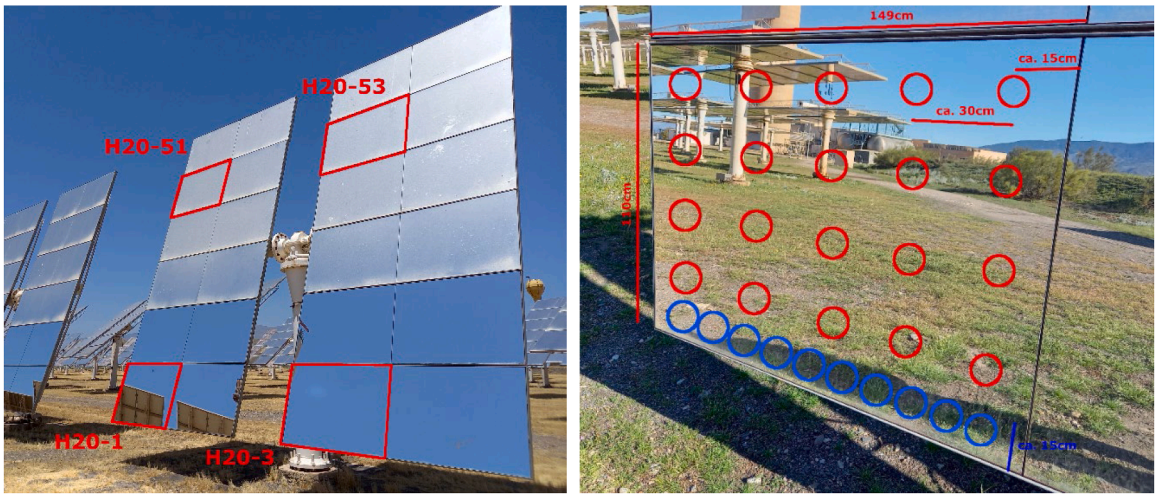

Fig. 4. Left: heliostat H20 with the measured facets marked in red (bottom line and higher line of extra campaign). Right: one of the measured facets during campaign with scheme of measurement spots (red: normal measurements, blue: extra measurements at lower edge).

cleanliness is defined as:

$$\xi = \rho_{soiled}/\rho_{clean} \tag{1}$$

The mean cleanliness over time, $\bar{\xi}$, is determined by the integration of the parameter over time, divided by the total measurement campaign duration. In this calculation, it is taken into consideration that the time between measurements is not the same for all periods, but slight deviations from the normal two-week period occur. Consequently, the equation used is not directly the average value of all measurements, but the formula presented in Eq. (2).

$$\bar{\xi}(t) = \frac{\int_{t=0}^{t} \xi dt}{\Delta t} \tag{2}$$

In reality, the number of measurements is limited and summation is used instead of integration. Every $\bar{\xi}_i$ is the mean value of cleanliness during the specific period and Δt_i the time between two measurements, Δt is the total time of evaluation as shown in Eq. (3).

$$\bar{\xi}(t) = \frac{\sum_{i=1}^{n} \bar{\xi}_i \Delta t_i}{\Delta t} \tag{3}$$

The soiling rate, *SR*, determines the decay in cleanliness over a given time period. Usually it is expressed in %/day, and it may change from day to day, depending on the environmental parameters at any given time. The *SR* is the most common parameter used to quantify soiling conditions for specific sites and use cases. The temporal resolution required for *SR* data depends on the use of the data. For certain tasks, such as O&M and the adaptation of soiling models, daily or higher frequencies may be desirable. As the cleaning frequency in commercial plants is in the order of one to two weeks, and because in this study an overall yearly comparison is being evaluated, the two-week measurement frequency is a compromise between effort and data accuracy. Since the measurement frequency for the main campaign is two weeks, a linear behavior is assumed between measurements, and *SR* is calculated according to Eq. (4) as the mean rate between measurements.

$$SR(t) = \frac{\xi_{before}(t) - \xi_{after}(t - \Delta t)}{\Delta t} \tag{4}$$

To evaluate the uncertainty of the measurement data, 95 % confidence intervals (*95 %CI*) are calculated, assuming a t-distribution of the data. The *95 %CI* are directly displayed together with the measurement data. To determine the uncertainty of linear fits used for device comparison and inclination influence, a Monte Carlo approach was used following recommendations in the Guide to the Expression of Uncertainty in Measurement [57,58].

2.4. Measurement campaigns

Two outdoor measurement campaigns were conducted for the here presented study. In addition, extra measurements were performed on small samples, to investigate certain additional key parameters and to perform measurements in the laboratory.

2.4.1. Main heliostat campaign

The main campaign comprises measurements during a whole year on the two selected heliostats, H18 and H20. During the campaign, the heliostats stayed in tracking mode during normal PSA operation times and went into stow position for the remaining time. Usual tracking time was from around 8:30 in the morning until 16:00 in the afternoon on weekdays only. Stow position was also used when wind velocity exceeded 50 km/h for safety reasons. The main parameters of the tracking times of the main and the extra campaign are given in Table 1. A detailed analysis of the daily tracking time changes was not included in this study. As there were few exceptions from the nominal times, the approximate tracking ratio for the two campaigns was calculated based on these parameters. For the main campaign the tracking to stow ratio is r_t=0.223. Two different stow positions were chosen for the heliostats to directly determine their influence on the soiling of the reflectors: the H20 heliostat was stowed with the reflective surface face-up and the H18 one face-down, both approximating horizontal positioning. The campaign lasted from April 2022 to April 2023 and thus covering a whole year and accounting for seasonal changes throughout the year, which can highly affect the soiling behavior.

The cleanliness of the heliostats was determined with the D&S-15R every two weeks before and after cleaning. Two facets on each heliostat were chosen on which the cleanliness was determined. In addition to the D&S-15R, measurements were performed with the Condor on three measurement days, to analyze variances in soiling determined with both devices for a range of soiling levels. The cleaning of the facets was performed manually by a crew of operators, using a pressurized jet of

Table 1
Tracking times during main and extra campaign.

Campaign	Tracking		Daily tracking time [hours]	Weekends	r_t [-]
	Start time (approx.)	End time (approx.)			
Main	8:30	16:00	7.5	Stop	0.223
Extra	Sunrise + 1 h	Sunset - 1 h	11	Continue	0.458

demineralized water applied with a HDS 10/20–4 M model manufactured by Kärcher (Winnenden, Germany) at a pressure of 100 bar, at ambient temperature, and a soft brush made of horsetail hair, until subjectively clean, to restore the initial reflectance. Cleaning duration and water use were not controlled but were adjusted by the operators. The complete recovery of cleanliness was verified by several measurements throughout the campaign of the reflectance taken after the cleaning tasks were performed. This verification was performed on three measurement days and the minimum absolute cleanliness achieved per facet on all these days was 0.999 after finishing the cleaning procedure—very close to the perfectly clean state and well in the limits of the measurement uncertainty. This allowed the omission of the measurements after cleaning for the rest of the campaign and thus avoided unnecessary extra work.

2.4.2. Extra heliostat campaign – extended tracking time

After completion of the main heliostat campaign and a preliminary evaluation of the data, an extra campaign was planned and executed. The same two heliostats and stow positions were also employed in this case. The main objective of the extra campaign is to determine the influence of extended tracking time on the soiling behavior, for the two stow positions. The daily tracking time (time ratio between tracking and stow) was increased compared to the main campaign. Tracking started at sunrise and ended at sunset, extending to work days and weekends and thus representing the maximum feasible tracking time for commercial power plants. This leads to a tracking to stow ratio for this extra campaign of approximately 0.458. Effective tracking times at commercial power plants are lower, due to factors such as operational strategies, cloud cover, maintenance and other unforeseen events [59–61]. Furthermore, the measurements of cleanliness at a higher distance from the ground were included in this campaign, as explained in chapter 2.3. The soiling at the two heights was evaluated after finishing the study of the extended tracking time.

The whole extra campaign comprises several operation and measurement periods between April 2023 and May 2024, with breaks in between periods and covering a total of approximately three and a half months. The rigid two-week measuring and cleaning schedule was not kept for this campaign, as a yearly soiling rate was not determined, but the focus was mainly on the effect of the higher tracking ratio on the soiling differences between heliostats.

2.4.3. Small reflector samples campaign

Two tasks were addressed measuring small reflector samples: (i) investigation of vertical stow and (ii) analysis of results compared to lab measurements of the solar-weighted near-specular reflectance. For that, several small reflector samples of 10 × 10 cm^2 size and the same material type of the heliostats studied, were also exposed during the execution of the research for the here presented campaigns. The small size of these samples was chosen to enable easy and flexible exposure and collection, at a site close to the main heliostats and to be able to perform measurements in the laboratory, with the equipment that has size limitations, namely the S2R reflectometer.

During the above presented main and extra campaign, the two extreme cases for the stow position were investigated, horizontally face-up and face-down. As many commercial designs of heliostats today don't have the capability for face-down stow, a simple estimation was performed on the potentially most favorable position for these heliostats: the vertical stow. Three samples were exposed during several weeks in 2024 on a fixed structure without tracking, close to the two heliostats, to investigate the difference in soiling of samples with vertical position, compared to the face-down position used in the heliostat campaigns. For these measurements, two samples were exposed vertically, one facing east and one facing west direction to eliminate the effect of wind direction on the soiling, and one sample was exposed face-down as the reference. This investigation was not carried out on the heliostats due to safety regulations, which prevent the long-term stow in vertical position, to avoid damage by higher wind velocities. At the PSA, during evening and night hours no regular operator crew is present, but only a minimal amount of personnel for strictly necessary tasks. At commercial plants, usually regular shifts are present 24 h a day, and this is why vertical stow may be feasible, if reaction to high wind speed situations is possible at all times. Samples were collected and measured with a frequency of roughly two weeks. The frequency was not kept strictly, as the data serves only as a comparison between the two cases, vertical and horizontal face-down. After collection, the reflectance was measured with the D&S-15R, followed by the re-exposure of the samples. Five D&S-15R measurements were taken on each sample and the average value calculated. The average value for the face-down and vertical case is then taken, the cleanliness values are calculated by division of the clean reflectance value and used for evaluation. For this campaign, data from five measurement days was collected.

To compare the results of the handheld field reflectometers to the more significant value of the solar-weighted near-specular reflectance, measurements of the latter had to be performed in the laboratory. To be able to determine the solar-weighted near-specular reflectance with the S2R, one small reflector sample was exposed for ca. two weeks and afterwards measured with the S2R, the D&S-15R and the Condor as explained in chapter 2.2. and an analysis of the differences in the results was performed.

3. Results & discussion

In this section, the results of all conducted campaigns are described. First, results on the homogeneity of the reflectance and soiling on the facets are presented, gained before and during the campaigns. Then the results of the main and extra campaign, followed by a comparison of the two are shown. The last part of this section details results on the additional parameters, investigated during the outdoor campaigns and the measurements on the small reflector samples.

3.1. Homogeneity of reflectance values on heliostat facets

The first step to conduct at the beginning of the experiments, was to determine the initial reflectance of the four facets used for the main campaign in the clean state to check possible degradation of the reflector materials. In Table 2, the average reflectance of the four facets is presented together with the standard deviations of the 20 measurements per facet. It can be seen that the average values differ only very slightly (difference of 0.1 %pt max) among facets and lie well within the measurement uncertainty of the equipment [62]. Some slight heterogeneity can be seen on the single facets, with the highest standard deviation of 0.4 % on facet 20–3. The small detected heterogeneities possibly stem from imperfect reflectance of the facet, as they already have been exposed in the field for a considerable time and secondly due to imperfect in-field cleaning. The good homogeneity of the initial clean reflectance assures a negligible influence of local reflectance variation on the average value in the soiled state.

As explained in Section 2.3, at the beginning of the campaign an experiment was conducted to investigate the influence of the number of measurements on the results of the mean reflectance determined per facet. The experiment consisted in the consecutive repetition of the normal 20 measurement-series per facet for four times on two facets with different soiling levels. As the exact measurement points vary from

Table 2
Initial reflectance of the four measured facets, facet mean and standard deviation.

Heliostat	Face-down		Face-up	
Facet	H18–1	H18–3	H20–1	H20–3
Reflectance ρ [-]	0.939 ± 0.001	0.939 ± 0.003	0.938 ± 0.002	0.939 ± 0.004

series to series, small variations between measurement series give indications on a high level of confidence in the obtained mean value. A relatively clean facet and a more soiled one were chosen for this experiment, to cover a wide range of soiling levels. For the stronger soiled facet, an additional fifth measurement series was conducted, increasing the number of measurements to 70 evenly distributed points on the facet, to analyze if more measurement points are needed when the soiling level increases. In Fig. 5, the results of the measurement series of both facets are displayed, presenting the mean values with the 95 % confidence intervals. It can be seen that only minimal differences exist among the mean values per facet of the different series, even for the heavier soiled one. The mean value of the four measurement series was calculated to be 0.934 and 0.864 for the two facets respectively, with standard deviations from this mean of 0.07 %pt and 0.14 %pt, respectively. The highest absolute variation detected was 0.21 %pt. Even the mean value for the series with 70 measurements is in good accordance with the other measurements (green bar in Fig. 5). These results indicate that a number of 20 measurements gives good estimation of the average facet reflectance. Also, no distinguishable trend can be detected for consecutive measurement series, which implies an insignificant influence of the measurement procedure on the soiling state, e.g. by contact between the reflectometer and the soiled surface.

To further investigate this topic, the influence of the soiling level on the homogeneity of the soiling was checked after completion of the main campaign, analyzing the values discussed in detail in Section 3.2. For this, in Fig. 6 left the standard deviations of the cleanliness measurements per facet are plotted over the mean values. It can be easily seen that the standard deviations in general are higher for heavier soiled facets, as expected. For highly soiled facets they can reach values over 12 %pt (points in the upper left corner of the graph), which means that soiling develops unevenly over the facet surface. Even for lower soiling levels, outliers can be detected due to unpredictable local conditions. For example, in Fig. 6 left one value for facet H18–1 shows a standard deviation over 6 %pt even at very low soiling conditions (blue dot on the upper right of the graph), which was due to an unusual soiling pattern on the lower left corner of this specific facet on that day (see Fig. 7). In general, for higher cleanliness values, standard deviations remain in the order of 2 %pt and lower.

As two facets were chosen per heliostat, it was also interesting to check the difference in cleanliness between these two facets of each heliostat. In Fig. 6 right, these differences between facets are displayed over the heliostat cleanliness. It can be perceived that such differences remain rather low, usually below 1 %pt with a maximum below 5 %pt. Higher differences usually appear at lower cleanliness values. The mean difference taking into account the whole campaign is 0.4 %pt, which indicates a low difference between the soiling of the facets located at the same height on the same heliostat.

3.2. Results of the main campaign

The main result data of this experiment are displayed in Fig. 8. Here, the cleanliness per heliostat is displayed over the whole main campaign duration in the upper graph, together with 95 % confidence intervals of the measurements. Taken into account are the 20 measurements per facet distributed over the surface of the facets, not including the extra values at the lower edges, which will be treated separately. The three graphs below show the main meteorological parameters during the campaign evolution. In the main graph, the blue line represents the face-down heliostat (H18) and the orange line the face-up heliostat (H20). The general behavior for both heliostats is a decline of the cleanliness between measurements every two weeks and the restoration of the cleanliness, by the applied cleaning afterwards. Few exceptions from this behavior can be seen in the graph. Firstly, after one month of the campaign start, cleaning was omitted one time to check for this influence of longer soiling periods without cleaning. Then, there are several periods with longer durations between measurements and respective cleaning actions. This was mainly in summer and winter due to vacation periods and respective lack of manpower to perform all tasks. Usually, throughout the year, the 2-week frequency was kept with a margin of around two days. Clearly visible is the behavior, that the face-up heliostat accumulates much stronger soiling, resulting in lower cleanliness values throughout the whole campaign. This is why the orange line lies much below the blue line for basically the entirety of the campaign duration. The face-up heliostat reaches levels of extremely low cleanliness even below 50 %, with an absolute minimum of 42.9 % cleanliness at the end of the dry summer period. The cleanliness reached for the face-down heliostat on the other hand keeps a moderately high level, with the absolute minimum value reaching 88.5 %. These results prove the superior protection from soiling by the positioning towards the ground. In this data, the dependence of the homogeneity of the soiling on the soiling level can be appreciated again, resulting in considerably higher confidence intervals for the face-up heliostat.

Even though a detailed analysis of the impact of the meteorological parameters on soiling behavior is out of the scope of this study, seasonal changes can be appreciated in the data with periods of stronger and weaker soiling. In general, during summer months soiling deposition is

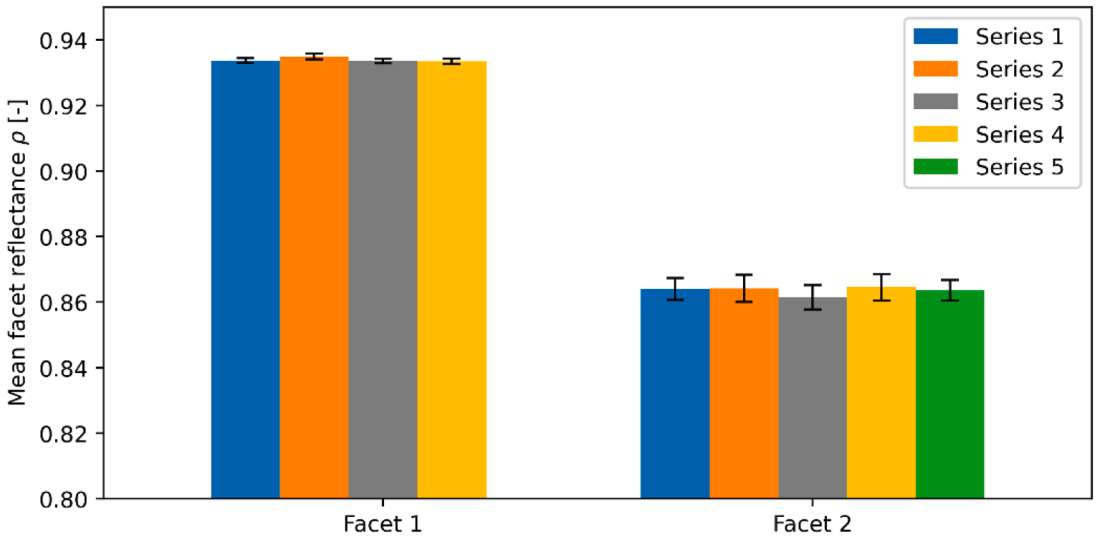

Fig. 5. Results of consecutive measurement series repeated on two facets.

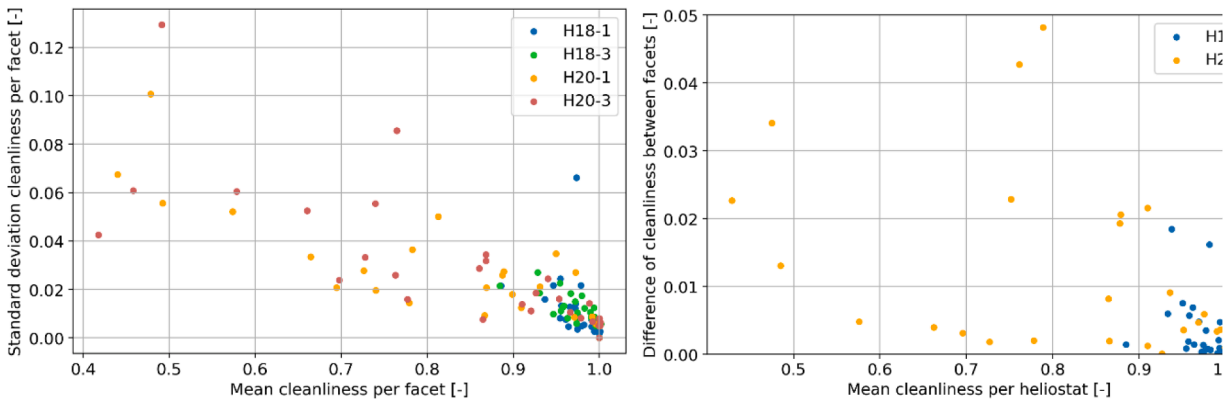

Fig. 6. Left: Standard deviation of measurements of single facets over the mean value per facet. Right: Difference of cleanliness between facets of the same height, over cleanliness per heliostat.

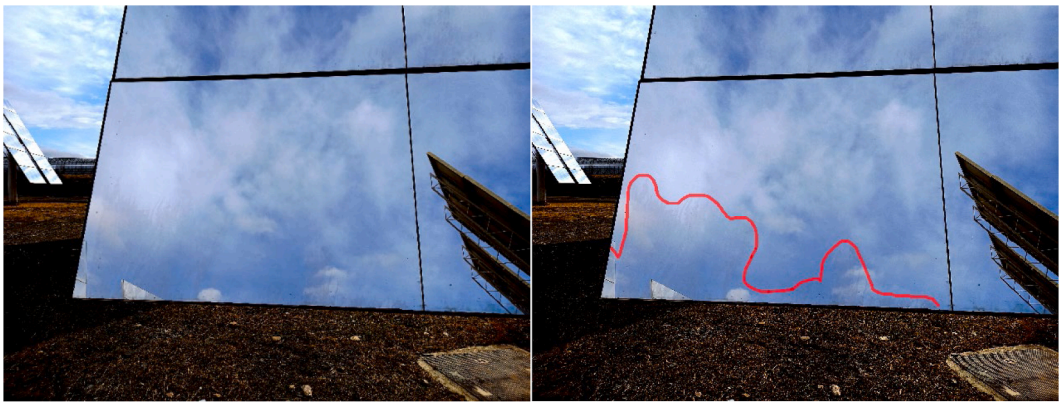

Fig. 7. Facet with heavily soiled pattern at lower left area of surface, right: original, left: marked area.

higher due to dryer atmospheres and higher particle concentrations in the air as previously reported in [11]. Winter and spring season show higher cleanliness levels mainly attributed to higher amounts of precipitation with the involved natural cleaning action, as reported in the literature [63]. For example, several precipitation events can be appreciated in the rain data in Fig. 8 at the beginning of the campaign, during the winter of 2023, and at the end of the campaign, coinciding with high cleanliness periods. In addition, some of the low cleanliness periods match with high average particle densities. Deviations from this behavior are common though, as soiling phenomenon are highly complex and can be influenced by single events such as higher dust loads or weak precipitations with soiling accumulation [64,65]. Especially the combination of particle density, wind speed and direction, as well as the orientation of the heliostat surface establish a complex behavior of the soiling of the reflectors, which has not been investigated here, and would probably require higher frequency soiling measurements.

In Fig. 9 the mean cleanliness is displayed for both heliostats over the campaign duration. This value gives an indication on the mean cleanliness of the respective heliostat during the campaign until this respective point in time. Final values of the curves give the evaluation of the whole campaign. Values of the mean cleanliness drop in the beginning of the campaign due to the increased influence of the more intense soiling. A minimum is reached for high soiling periods and then a slight recovery during low soiling season is detected in accordance with data in Fig. 8. Again, the lower overall cleanliness for the face-up heliostat can be appreciated. After the initial stabilization phase, the mean cleanliness stays roughly 10 %pt lower for the face-up heliostat compared to the face-down one. Final values in the curve corresponding to values representing the mean cleanliness of the whole campaign year are $\overline{\xi} = 0.895$ for face-up and $\overline{\xi} = 0.984$ for face-down, presenting a difference of $\Delta\overline{\xi} =$ 8.9 %pt between both. The evolution of the curves over the campaign duration underlines the importance to conduct this kind of studies for at least a whole year, to achieve representative results.

As explained in the introduction, a parameter often used to characterize sites and specific conditions regarding soiling, is the soiling rate, to evaluate daily losses, which is expressed as %/day. The soiling rates for the main campaign are presented in Fig. 10 and in accordance with the above presented data, soiling rates are always higher for the face-up heliostats, even though the values vary strongly over time for both heliostats. The face-up heliostat presents a mean soiling rate calculated for the whole campaign of SR=1.4 %/day with a maximum of 4.8 %/day, and the face-down heliostat shows a mean of SR=0.2 %/day with a maximum of 0.8 %/day. This means, the mean soiling rate reaches a value approximately 7 times higher for the face-up stow case. To get more accurate soiling rate data, it would be interesting to perform measurements at higher frequency, to really show daily changes in soiling behavior. For long term campaigns this entails a high workload though, if measurements are not performed by autonomous sensors.

The lower soiling rate of the face-down stow operation directly translates to a higher average cleanliness of the solar field. Supposing an O&M strategy with cleaning at a defined cleanliness threshold, this would directly result in fewer cleaning procedures per year. To give a very simplistic economic analysis, the sevenfold reduction in soiling ratio leads to a sevenfold reduction in cleaning and the related costs. As an example, this analysis is performed with data from [32], where annual cleaning costs are given for a 50 MW CSP plant in Spain. These costs could be reduced by 85 % according to the analysis, resulting in absolute savings in cleaning costs of ca. 205 k€/a. This may only be valid

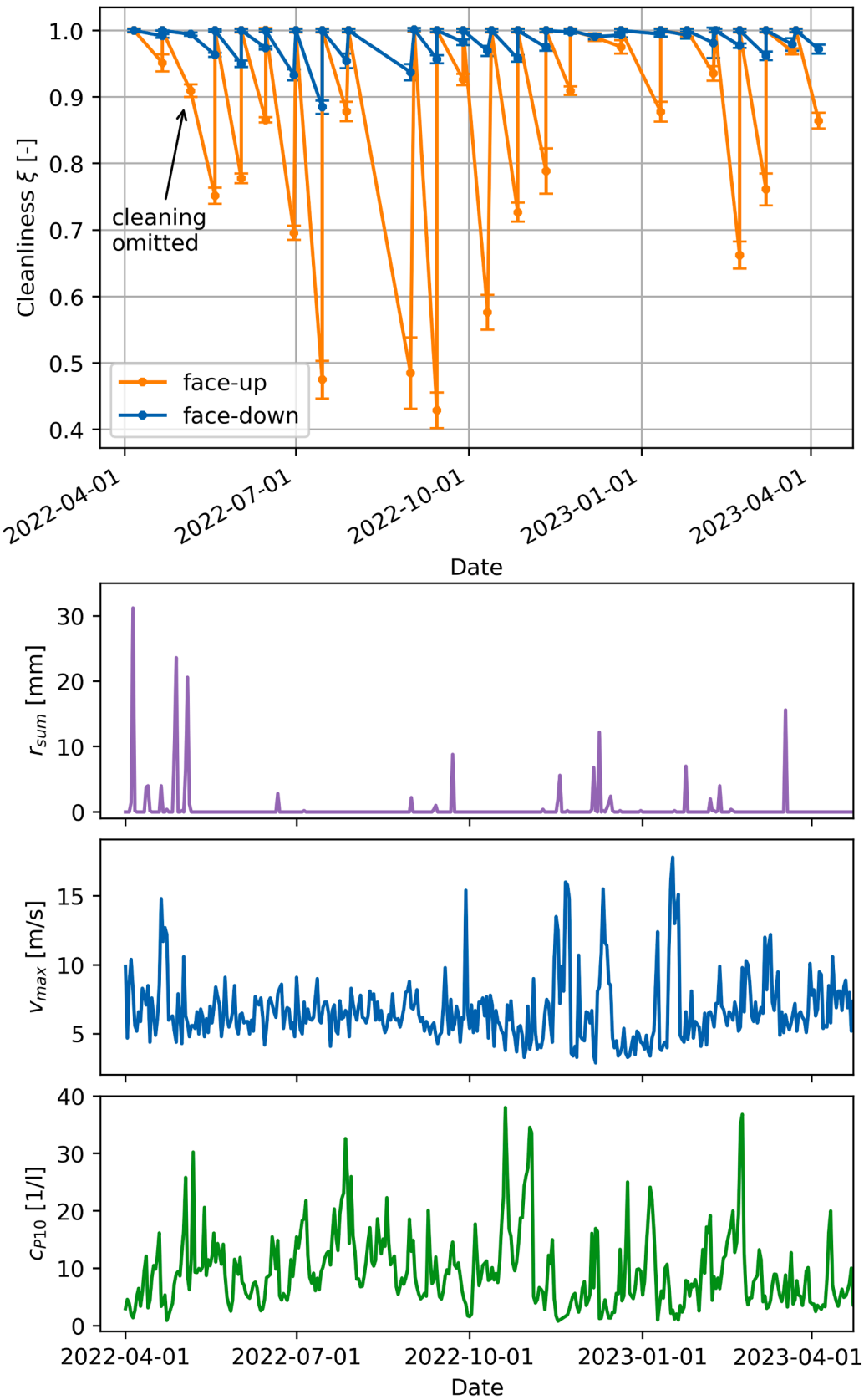

Fig. 8. Main graph above: Cleanliness of both heliostats over the whole campaign duration, with grey vertical lines marking 3-month periods. Three graphs at the bottom: daily precipitation sum, maximum wind velocity and average particle density.

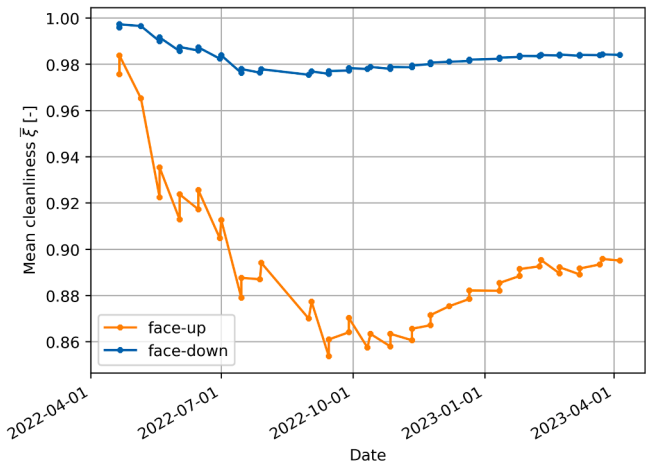

Fig. 9. Mean cleanliness per heliostat over campaign duration, final values represent values to be evaluated for whole campaign.

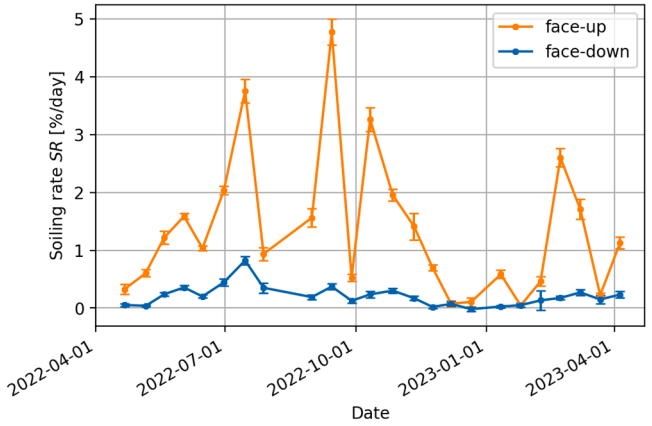

Fig. 10. Soiling rate SR over the whole main campaign duration for both heliostats.

if cleaning costs decrease linearly with cleaning actions (or with square meter cleaned per year). Also, the additional costs of the face-down stow options have to be weighed, which would highly depend on the specific heliostat and solar field design. Some of the factors including these extra costs include heliostat drives, reduced reflective area, density of the solar field and total field size in relation to the receiver size and storage strategy.

The results presented for this main campaign offer reliable data for the PSA and the investigated technology configuration. The data may be used for this site directly to adapt the O&M strategy if necessary and could be of use when new heliostats are installed, to assess the necessity of a face-down stow possibility. Since soiling is a site specific parameter, results for other sites are expected to vary considerably in absolute numbers for the difference between stow positions. On the other hand, it is expected that relative differences will be similar at other sites, if the underlying soiling processes, determined largely by vertical settling of dust particles, are not completely different. It should be verified in the future if this hypothesis holds, with long-term data from alternative sites.

3.3. Results of the extra campaign

The cleanliness data of the extra campaign, conducted from April 2023 to May 2024, with breaks, comprising an exposure time of roughly seventeen weeks, is presented in Fig. 11. The gaps between the different periods of the campaign without measurements, are not displayed for the ease of visualization. As for Fig. 8, for comparison, the evolution of the main meteorological parameters is included alongside the cleanliness. The principle behavior of the main campaign is detected for the extra campaign as well: the face-up heliostat shows a lower cleanliness than its face-down counterpart. But for this campaign the differences are less extreme than for the main campaign, with the y-axis range being the same as for Fig. 8. A direct comparison of the absolute values of the mean cleanliness and soiling rate to the main campaign has to be taken with caution, because the extra campaign does not comprise a whole year. But the relative difference gives an indication of the contrast to the main campaign. The mean cleanliness for the face-up and face-down heliostat of the extra campaign are $\bar{\xi}$=0.919 and $\bar{\xi}$=0.954, respectively. This is only a difference of $\Delta\bar{\xi}$=3.5 %pt compared to $\Delta\bar{\xi}$=8.9 %pt from the main campaign. The absolute minimum values of cleanliness for the extra campaign are 73.8 % and 85.7 % for the face-up and face-down, respectively. The soiling rate during this campaign was calculated for all periods in which after and before cleaning values exist, totaling a number of five periods. The resulting mean soiling rates are SR=0.7 %/day for the face-down and SR=1.2 %/day for the face-up heliostat, presenting a ratio between rates of 1.6. Hence, mean cleanliness as well as soiling rate differences between heliostats are lower for this campaign, compared to the main one. A clear relation to the meteorological parameters is not visible. The lower cleanliness during the middle part of the campaign may be influenced by the higher particle density present during this period, while the higher cleanliness of the last part may be influenced in part by the rain events. As for the main campaign, a more detailed investigation would have to be performed to gain further insights on these influences.

3.4. Campaigns comparison – tracking time ratio

The cause of the lower differences between the heliostats, with respect to the main campaign, lies in the ratio between the time the heliostats are placed in stow and tracking position. To estimate the ratio for both campaigns, the weekly operation is taken into consideration. For the main campaign, the heliostats are in tracking 5 out of 7 days with approximately 7.5 h per day. This results in a tracking to stow ratio of 0.223 for the main campaign. During the extra campaign, the heliostats are in tracking mode 7 days a week with approximately 11 h per day, resulting in a tracking to stow ratio of 0.458, roughly doubling the one from the main campaign. This means, that in the main campaign the heliostats experience a longer time in stow mode, which is the mode where discrepancies between both heliostats arise from, and this results in bigger differences in soiling behavior between the heliostats for the main campaign.

To make a direct comparison between the cleanliness of the two heliostats, in Fig. 12 the cleanliness of the face-up heliostat is presented on the y-axis against the face-down one on the x-axis for both campaigns, the regular (blue dots) and the extra (red dots) campaign. There are more data points for the regular campaign due to its longer duration. The general tendency is clear for both campaigns: the lower the cleanliness for one heliostat, the lower it is for the other. But, for the extra campaign the differences between heliostats are less extreme. This can be seen, because the data points for the extra campaign are closer to the grey horizontal line representing equality between heliostats. Least square fitting of a linear relationship between heliostats can be performed, to evaluate the trends for both campaigns. A linear trend can be appreciated, but the data scatters significantly. This scattering is due to the fact that the soiling of the heliostats is complex and time dependent, but not a sign for low quality of the data. While in general, periods of strong soiling affect both heliostats, the concrete soiling events can take place during tracking or during stow. When they happen during tracking, the influence on both heliostats is the same or similar, while when they happen during stow, the face-up heliostat is affecter more strongly. A detailed analysis for each period between measurements, of

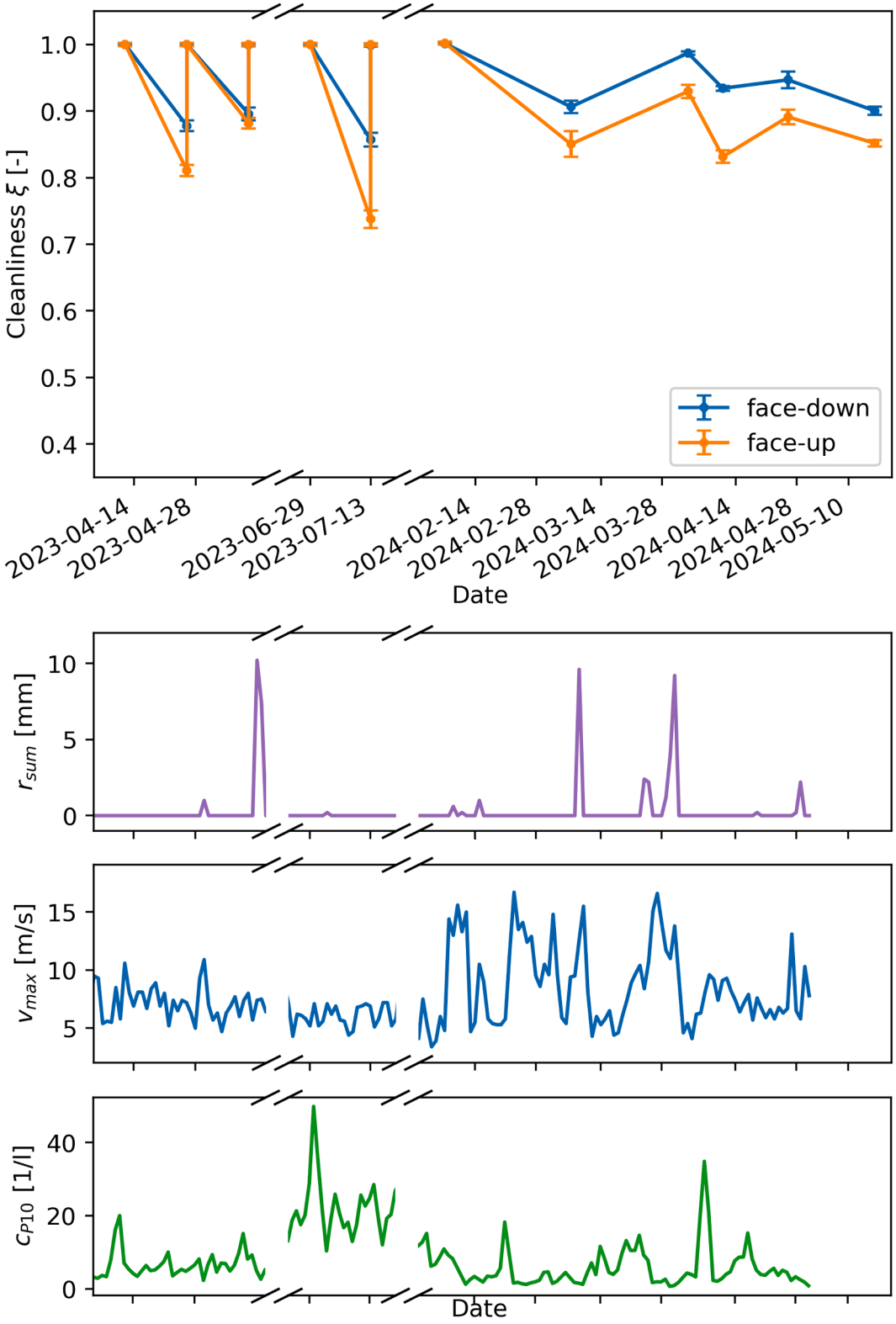

Fig. 11. Main graph at the top: Cleanliness of both heliostats over the whole duration of the extra campaign with gaps during several months of down time. Three graphs at the bottom: daily precipitation sum, maximum wind velocity and average particle density.

the environmental parameters (precipitation, wind, etc.) may lead to an explanation of the scattering for the single data points. For the sake of simplicity, taking into account a linear relation between the cleanliness of both heliostats, the difference between the two campaigns is clearly visible. R^2 values for the campaigns of 0.72 and 0.90 for the normal and extra campaign, respectively, show this linear relation with considerable scattering. The higher R^2 value of the extra campaign indicates better linear correlation with less scattering, which may be explained by the longer time the heliostats stay in tracking and with this less time in stow, with less possibilities of differences in the behavior. The slope of the

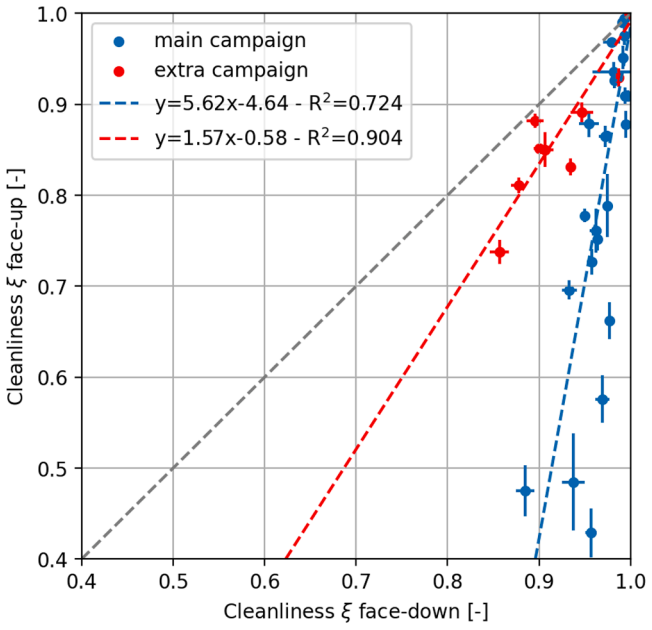

Fig. 12. Cleanliness of face-up stow heliostat against face-down stow heliostat for main and extra campaign together with linear trend line for correlations.

linear trend lines indicates the difference from equal behavior of both heliostats. A value of 1 corresponds to the same behavior for both heliostats and the higher the value, the stronger are the differences. Here the main campaign has a slope of 5.62 and the extra campaign results in 1.57. With these trend lines it is possible to quantify the advantage in soiling reduction by face-down stow for the two investigated tracking ratios. It has to be kept in mind that the data of the extra campaign do not comprise a full year and thus contains higher uncertainty. The two campaigns represent two extreme cases in relation to tracking time, as the main campaign used tracking times much shorter than expected for commercial plants, while the extra campaign used daily tracking close to the natural upper limit set by sunrise and sunset. Operation in a commercial power plant would entail tracking ratios in between the two here presented. A simple estimation can be performed, knowing the tracking time of a specific site and interpolating between the here determined values. For example, as a first approximation, and keeping in mind that only two data points (corresponding to the two campaigns) are available, it can be assumed that the relation between tracking ratio and soiling rate is linear. With the two tracking ratios (0.223 for the main campaign 0.458 for the extra campaign) and the two yearly average *SR* ratios between face-up and face down (7 for the main campaign and 1.6 for the extra campaign), a linear equation can be established to calculate the *SR* ratio to $SR_{up}/SR_{down} = -23.0*r_t+12.1$. This way an interpolation can be performed to determine the advantage in *SR* for intermediate tracking ratios. It has to be stressed that this relationship should be verified by including at least three measurement campaigns including a whole year of data at different tracking ratios and to find out its limitations.

3.5. Additional parameters

This section presents the results obtained during the experiments, concerning the influence of several additional parameters (distance to the ground, area of the facet, measurement equipment and surface inclination) on the soiling behavior of the heliostats.

3.5.1. Influence of facet height on soiling

On five measurement days of the extra campaign, reflectance measurements were performed at an additional height apart from the lowest facet line, approximately 6 m above the ground as explained in the methodology. The data of these measurements is revealed in Fig. 13. Displayed is the difference in cleanliness between the lower and the upper line of a heliostat, versus the mean reflectance of this heliostat. This is done for both heliostats. Negative values represent a higher cleanliness at the upper line compared to the lower and vice versa. Apart from two outliers, all values are negative, with a trend of larger differences with higher soiling levels, i.e. lower cleanliness. The outliers indicate a strong scattering of the data due to heterogeneous soiling distribution over the heliostat area. 95 %CI is quite high for these measurements and for cleanliness values above 0.85 the differences are close to zero with 95 %CI including the zero value. But at lower cleanliness values the difference is negative and statistically significant (95 % CI not including zero difference). The mean value of all differences is 1 %pt with a maximum difference of 3.5 %pt at a cleanliness level of 0.738. This shows, that soiling is stronger closer to ground for this campaign, but the influence on the overall heliostat cleanliness is negligible. In addition, these differences are expected to be lower for the main campaign, as the time in tracking is lower, which is when the differences in height really do develop.

3.5.2. Edge soiling effect

In the graphs of the sections above, the cleanliness of the facets is shown, meaning the cleanliness determined on the measurement spots evenly distributed over the whole facet surface (labeled here as “facet measurements”), but excluding the extra measurements on the lower facet edges (labeled as “edge measurements”), as explained in Section 2.3. These edge measurements were performed to understand the influence of the heterogeneous soiling patterns detected there in the past. In Fig. 14 the differences in cleanliness between the facet cleanliness and the edge cleanliness are displayed for the whole normal campaign together with the 95 %CI of the single measurements. Negative values mean that the lower edge is more soiled than the overall sample surface. As can be seen, the lower edges are usually soiled stronger than the overall surface. Except for few low soiling levels at the beginning of the campaign, values remain negative throughout the whole campaign. Typically, the differences are higher for the face-up heliostat due to its higher general soiling levels. Few exceptions can be detected, where the differences are higher for the face-down heliostats. The hypothesis to explain the different soiling pattern on the lower edge is that accumulation of water and moisture concentrates at these lower edges, due to gravity. This effect strongly depends on the inclination of the heliostat in combination with the water present on the facet at that concrete point in time. The mean differences in cleanliness between edge and facet, calculated over the whole campaign duration are 5.2 %pt and 3.2 %pt for the face-up and face-down heliostat, respectively, resulting in an overall difference of 4.2 %pt.

As the size and homogeneity of this soiled lower edge varies strongly, this effect is not taken into consideration for the overall evaluation. To give an estimation on the possible magnitude of this effect, a simplified analysis is performed. A series of eight randomly selected images was taken during the main measurement campaign, selecting facets with clearly visible differences in soiling between lower edge and area, to have a statistic evaluation. The images are treated with an image processing software to divide by edge and the rest of the facet area. This process is prone to uncertainties because it depends on manual selection by the user and the areas of facet and edge soiling are not always well divided. Then, the area ratio between edge and the whole of the facet is calculated. Two examples of this selection can be seen in Fig. 15. On the left, the soiling pattern of the whole facet is displayed and on the right the marked area in red is the edge soiling. The full dataset with all evaluated images can be found in the supplementary material. The mean ratio of edge to facet area for all 8 images is 9.8 % with a standard deviation of 4.3 %. With the mean of cleanliness differences calculated above, of 4.2 %pt, the difference for each image can be calculated of taking the edge soiling into consideration or not. The resulting mean

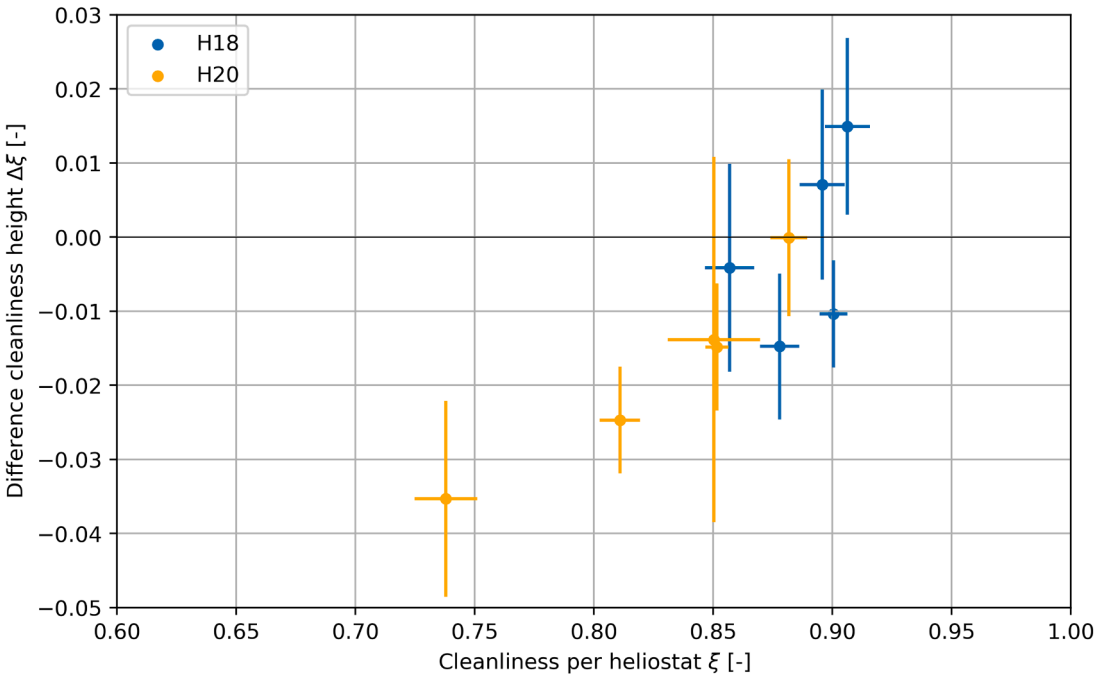

Fig. 13. Plot of differences cleanliness between height over cleanliness per heliostat.

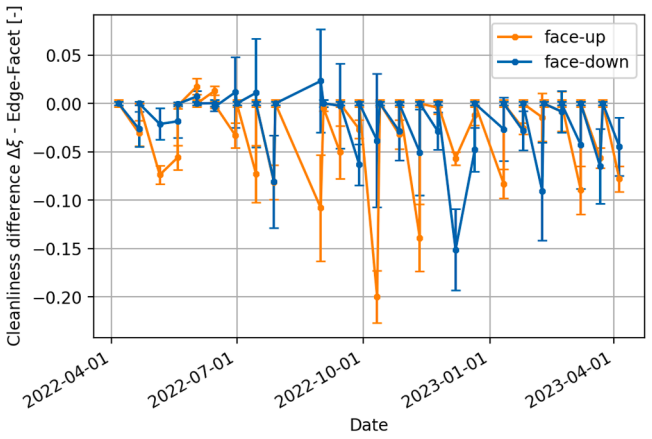

Fig. 14. Differences in cleanliness between the measurements of the whole area of the facets and the lower edge, both heliostats.

difference in cleanliness of the cases for all images is 0.4 %, which is relatively small compared to the overall difference between stow positions of $\Delta\bar{\xi}$=8.9 %pt. This is why the effect of the heterogeneous soiling patterns on the total cleanliness is neglected for this study.

3.5.3. *Influence of the measurement device*

To make an estimation of the influence of the used measurement instrument and parameters on the total value of reflectance and cleanliness, a sample of a similar 4 mm silvered-glass reflector material was exposed outdoors for a short period of approximately two weeks and afterwards measured with three different techniques, as explained in 2.2: the D&S-15R used for the whole outdoor campaign, the alternative Condor reflectometer and the S2R lab equipment. For the S2R, spectral and solar-weighted reflectance is presented at θ_i=15°, as near-normal similar to the portable reflectometers, and θ_i=30°, as a realistic value for the mean angle in the PSA heliostat field over the year. The acceptance angle selected was φ=12.5 mrad, representative for PTC and CRS technologies. The measured sample exhibited a cleanliness value of 0.699 measured with the D&S-15R and thus represents a heavily soiled state. In Fig. 16, the near-specular reflectance spectrum determined with the S2R, is presented together with the values measured with the portable reflectometers. At higher wavelengths close to 2500 nm, the S2R shows a higher noise level, especially at θ_i=30°, which does not affect the measurements in the more relevant rest of the spectral range. As can be observed, the D&S-15R value agrees well with the S2R values at θ_i=15°, due to the same utilized acceptance angle. The value for the Condor is higher due to its higher acceptance angle and the related higher amount of scattered light to enter its sensor. S2R values at 30° are slightly lower than at 15° due to a larger scattering at high θ_i [66].

As explained in the introduction, the solar-weighted near-specular reflectance is the most significant value determining the optical quality of the reflectors. It is determined by weighting the spectral measurement of the S2R with a standard solar spectrum. In Table 3, the calculated solar-weighted value from the S2R is compared to the reflectometer values. While in the graph above, the D&S-15R hits the spectral S2R value at 660 nm at θ_i=15°, a difference of 2.3 %pt to the solar-weighted value at 30° is detected. The difference of the Condor value to the S2R is considerably higher with 14.9 %pt, which can be explained again by the higher acceptance angle of the Condor device and the corresponding underestimation of the soiling.

As the measurement of this one sample represents the case of very strong soiling, these differences are expected to be much lower for the overall campaign as well as for operating conditions. The higher the cleanliness, the lower the scattering of reflected light is expected and with this, the influence of the acceptance angle on the measurements, until reaching a cleanliness value of 1 for all devices. To make an estimation of the effect of the equipment selection on the overall campaign, linear behavior is assumed of the correlation between devices. Then, with this data it can be calculated, what value of S2R and Condor correspond to each D&S-15R value. This was done for the campaign mean values of cleanliness for both heliostats presented above. The corresponding mean cleanliness values are displayed in Fig. 17. Here, for the cleanliness levels of the two heliostats, the differences to the most significant reference value (S2R) of both field reflectometers can be evaluated. For the face-up heliostat, the differences to the S2R value are 0.5 %pt and 5.1 %pt for D&S-15R and Condor, respectively. For the face-down heliostat they are 0.1 %pt and 0.8 %pt. Also, the differences between heliostats can be calculated depending on the used equipment.

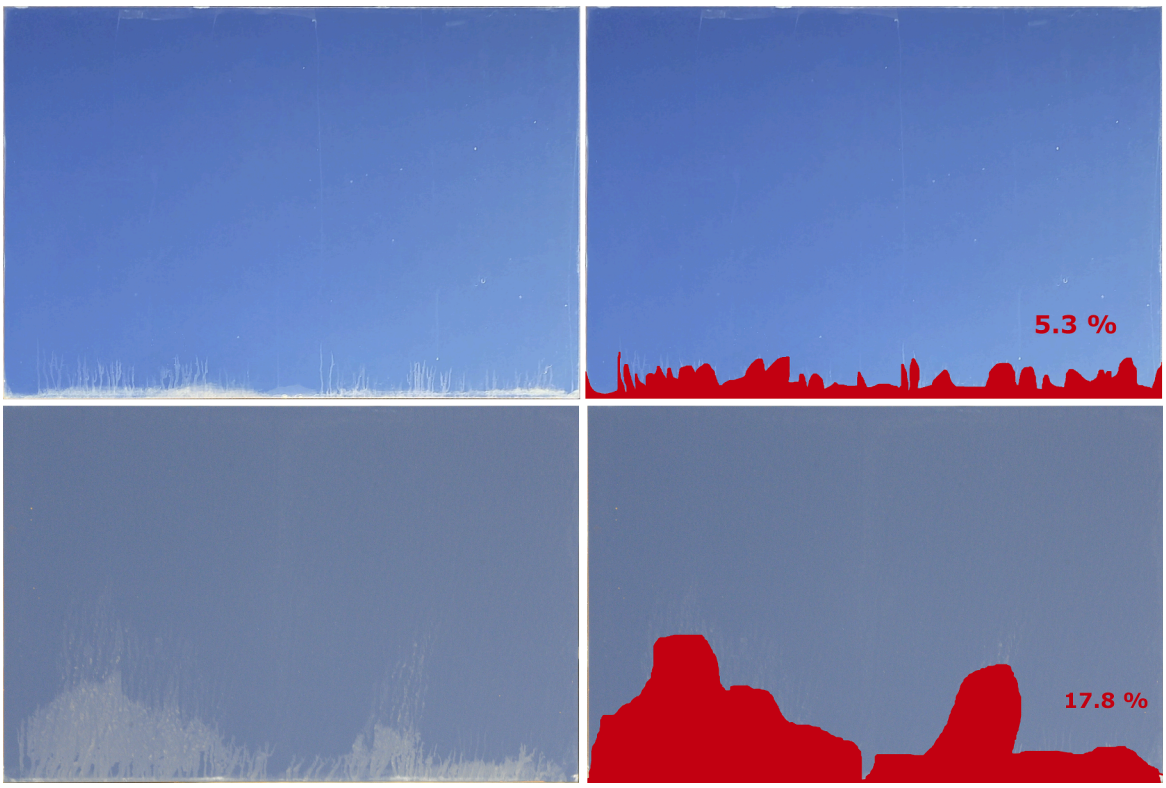

Fig. 15. Images of soiled facets (2 examples) with clearly distinguishable lower edge soiling pattern. Left: original images, right: marked soiled edge area in red, with percentage of edge pattern to total facet area.

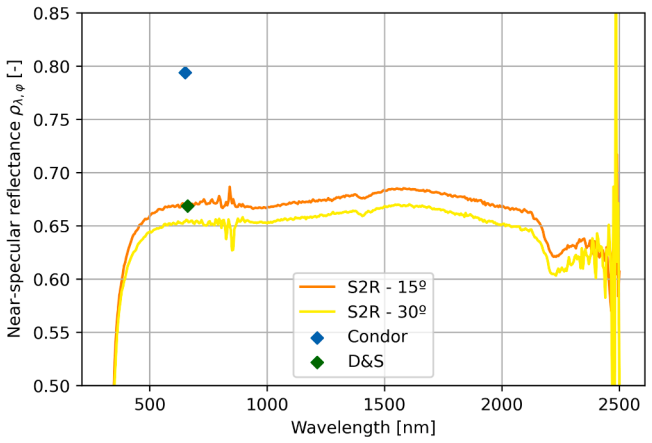

Fig. 16. Reflectance measurements of the small reflector sample in soiled state with different measurement devices (S2R, D&S-15R, Condor), different reflectance parameters: spectral specular reflectance at θi=15° and 30° (S2R), monochromatic specular reflectance at θi=8° and φ=12.5mrad (D&S-15R), and θi=12° and φ=145 mrad (Condor).

Table 3
Reflectance values of soiled sample determined with different devices, included the difference to S2R reference value.

	Reflectance		
Device	S2R (30°, 12.5 mrad)	D&S-15R	Condor
Reflectance	0.645	0.669	0.794
Difference to S2R	-	0.023	0.149

While the difference between face-up and face-down are similar for S2R and D&S-15R, 9.3 %pt and 8.9 %pt, it is much lower for the Condor with 5.0 %pt. This means both portable devices underestimate the soiling influence, with a larger underestimation in case of the Condor. Overall, the values measured with the D&S-15R are much closer to the real value than the ones determined with the Condor. But when the correlations between the devices are known, the reflectometer values can be transferred to the corresponding true value. This should be taken into account, when decisions are taken or calculations are performed for O&M strategies or yield estimation.

To further investigate the relation between measurements with the different devices and the behavior during outdoor exposure, Condor measurements were performed in parallel to the D&S-15R ones, on three days during the main campaign. The collected measurement data comprises a total of 7 facet measurements. In Fig. 18 the mean reflectance per facet is displayed, measured with the Condor over the values measured with the D&S-15R (green data points) together with the 95 % CI of the data. The corresponding value of the above presented small sample is included here as well (yellow point). The linear correlation assumed for the estimation above could be confirmed here. The linear trend line between measurements is displayed in the graph as well, together with the linear correlation coefficient of R^2=0.9999 and the confidence interval of the trend line. The R^2 very close to 1 confirms the linear behavior, with little scattering, and even the data point from the extra sample is close to the trend line. The relatively wide confidence interval indicates that the uncertainty of the trend line coefficients is large, which could be reduced by a campaign including more data points. While the differences between reflectance of the two devices, and with that cleanliness, are considerable and rise with heavier soiling, the linear correlation makes it possible to easily translate measurements with one device to the other. That means, if data is available of one reflectometer, but for further calculations, values of the other are of interest, for example due to another acceptance angle for yield analysis, the correlation can be used to determine the other reflectometer data. As

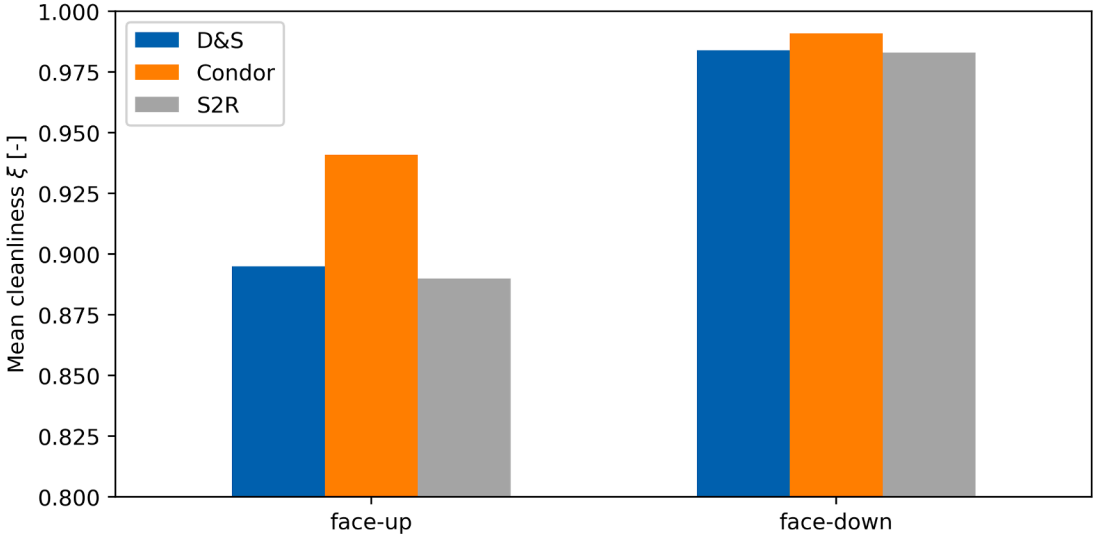

Fig. 17. Mean cleanliness values for heliostats of the main campaign, measured value for D&S and estimated values for S2R and Condor based on linear correlation between devices.

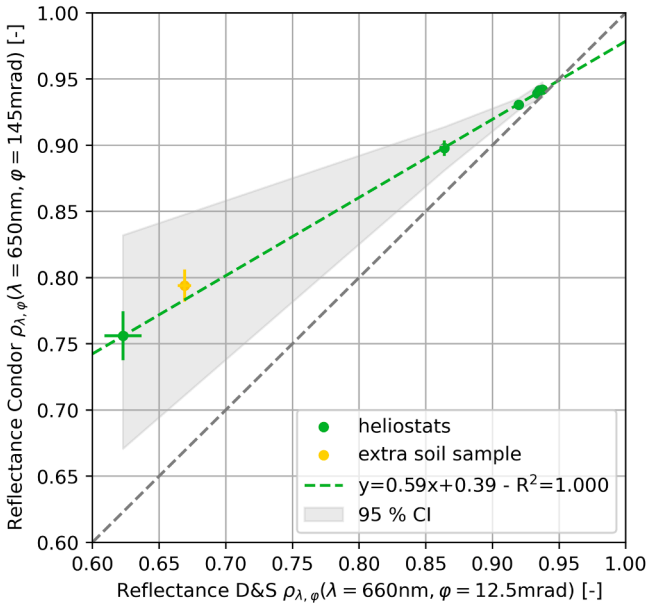

Fig. 18. Reflectance measured with the Condor vs. D&S-15R, main campaign data and small sample together with linear approximation of main campaign data points.

data from various days throughout the campaign is included here, it seems that seasonal changes don't have an effect on the correlation. Additional confidence in the correlation comes from similar results published by Sansom et al. [25] from measurements at a PSA PTC. In that publication D&S-RGB was displayed over Condor and not vice versa. The linear correlation was found to be $y_{D\&S} = 1.78\ x_{Condor} - 0.74$, compared to the one found here to be $y_{D\&S} = 1.69\ x_{Condor} - 0.66$, which agree very well, considering differences in campaign design and execution. For future use, it is recommended to further investigate the limitations of the correlation, especially concerning site dependence, type of soiling, further devices, etc.

3.5.4. *Influence of reflector surface inclination*

As explained in Section 2.4.3 of the methodology, to compare the face-down position, the ideal case in terms of soiling protection, to the most favorable alternative, the vertical stow, small reflector samples were exposed on a fixed rack. Results of this study are presented in the following. In Fig. 19, the cleanliness of the vertical samples is compared to the face-down sample. This data cannot be directly compared to the data presented in Fig. 12 for the main and extra campaign, as no tracking was involved here, but only serves as an estimation. The position was fixed during the whole exposure duration. Consequently, the data only serves to make an estimation on the direct comparison between the two cases of face-down and vertical. Assuming a linear behavior, it can be seen that the soiling is more than twice as high for the vertical case compared to the face-down case. That means that vertical stow shows a better protection against soiling compared to horizontal face-up stow, but does not reach the protection level of face-down stow. To better quantify differences and benefits of vertical compared to face-down, it is recommended to conduct additional measurements on full-size heliostats during operation, similar to the above presented main campaign, for a site of interest. Ideally such a campaign would directly compare the

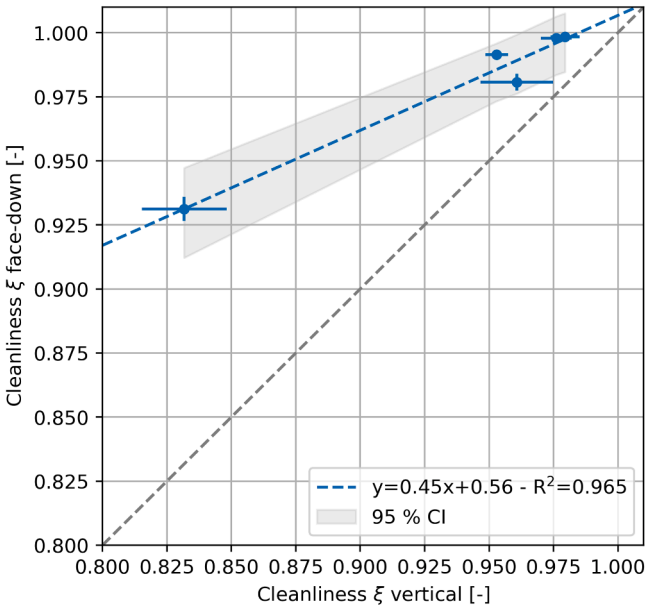

Fig. 19. Cleanliness of the face-down sample over the vertical sample, with linear trend line of data.

vertical stow on tracked heliostats to an alternative case such as the face-up stow, as in the here presented main campaign. To conduct this campaign at the PSA a 24 h safety protocol would have to be in place, including an extended operator crew or a fail-proof automatic control system that avoids failure during high wind periods by placing the heliostat in a safety position. Alternatively, the use of advanced soiling models could be investigated, which include detailed behavior of soiling for surface inclinations depending on the meteorological parameters.

4. Conclusions

This research investigates the influence of the stow position heliostats are placed in during inactivity, on the soiling of the heliostat reflectors. It was shown that for the here used site and operational parameters, face-down stow presents a clear advantage in relation to soiling protection compared to face-up stow. Over a whole representative year, this results in a considerably higher mean cleanliness of the face-down stow option with $\overline{\xi} = 0.984$ compared to face-up $\overline{\xi} = 0.895$, presenting an absolute difference of $\Delta\overline{\xi} = 8.9$ %pt. Hence, soiling rates for this case are nearly seven times lower for face-down with 0.2 %/day compared to 1.4 %/day for face-up stow. In commercial CSP plants, often cleanliness thresholds are used to make cleaning decisions. Based on that, the face-down stow would directly lead to a sevenfold reduction in annual cleaning effort. Differences were found to be smaller for alternative cases with varying parameters, especially reduced stow-to-tracking time ratio. In an extra campaign with much higher daily tracking time, the difference between stow positions decreased to an absolute mean cleanliness difference of $\Delta\overline{\xi} = 3.5$ %pt and a 1.6 times lower soiling rate for face-down stow. During operational conditions in commercial plants with common tracking times, these parameters are expected to lie in between the two investigated extreme cases. In addition, the evaluation highlighted the importance to cover an entire year, to produce significant soiling results in this type of campaigns. This data may serve as an input parameter for future design choices for heliostats and decisions on operational strategies.

During the execution of the campaigns, the influence of further secondary case specific parameters was analyzed. It was concluded, that the face-down position has a clear advantage compared to the other common beneficial position of vertical stow, in terms of soiling prevention. A slight dependence of the soiling on the height above ground was detected. Mean differences between facets close to the ground and on the upper edge of the heliostats are <1 % and can be neglected, when the differences between heliostats are analyzed. Local heterogeneous soiling patterns may present considerable differences in reflectance, but the influence on the overall facet cleanliness during this study resulted in a negligible cleanliness difference of 0.4 % and is thus neglected for the main evaluation. In general, reflectance heterogeneity increases with stronger soiling levels, but using the mean of 20 reflectance measurements per facet, has proven to give a good estimation of the average facet cleanliness.

The selection of the utilized reflectometers for the soiling determination plays an important role and may influence the gained results considerably. Commercial portable reflectometer devices vary in the measured reflectance parameters used and modification in the acceptance angles and wavelengths have an impact on the results. For this study, two of the most common commercial reflectometers were used successfully and it was possible to determine simple linear correlations between the different devices, which permits the translation of results of one equipment into the other. Further research into the applicability of these correlations and their limits is recommended.

CRediT authorship contribution statement

Johannes Wette: Writing – original draft, Visualization, Methodology, Investigation, Formal analysis, Data curation. **Florian Sutter:** Writing – review & editing, Supervision, Methodology, Conceptualization. **Raúl Enrique-Orts:** Writing – review & editing, Resources, Methodology, Conceptualization. **Manuel Pérez-García:** Validation, Supervision, Conceptualization. **Ricardo Sánchez-Moreno:** Project administration, Methodology, Investigation. **Aránzazu Fernández-García:** Writing – review & editing, Validation, Supervision, Methodology, Investigation, Funding acquisition, Formal analysis, Conceptualization.

Declaration of competing interest

The authors declare that they have no known competing financial interests or personal relationships that could have appeared to influence the work reported in this paper.

Supplementary materials

Supplementary material associated with this article can be found, in the online version, at doi:10.1016/j.rineng.2025.107890.

Data availability

Data will be made available on request.

References

[1] C. Ransom, State of the Climate 2024, UNO - World Meteorological Organization, 2024.
[2] K. Schwab, T. Malleret, The Global Risks Report 2025, World Economic Forum (2025).
[3] O. Ališauskas, World Energy Outlook 2024, IEA (2024).
[4] Renewable capacity statistics 2024, IRENA, Abu Dhabi, 2024.
[5] C. García-Baños, M. Blanco, C. Prieto, M. Silva, Renewable Energy benefits: Leveraging local Capacity For Concentrated Solar Power, IRENA, Abu Dhabi, 2025.
[6] M. Bülow, R. Pitz-Paal, Energy and Climate change, in: T.M. Letcher, V. M. Fthenakis (Eds.), Status and Perspectives of Concentrating Solar Technologies, Academic Press, 2025, pp. 251–277, https://doi.org/10.1016/B978-0-443-21927-6.00017-9.
[7] M. Osman, I. Qureshi, Review of Photovoltaic and Concentrated Solar technologies including their performance, reliability, efficiency and storage, Results. Eng. (2025) 104424, https://doi.org/10.1016/j.rineng.2025.104424.
[8] K. Zereg, A. Gama, M. Aksas, N. Rathore, F. Yettou, N. Lal Panwar, Dust impact on concentrated solar power: a review, Environmental Engineering Research 27 (2021), https://doi.org/10.4491/eer.2021.345, 210345–0.
[9] P. Bellmann, F. Wolfertstetter, R. Conceição, H.G. Silva, Comparative modeling of optical soiling losses for CSP and PV energy systems, Solar Energy 197 (2020) 229–237, https://doi.org/10.1016/j.solener.2019.12.045.
[10] K. Ilse, L. Micheli, B.W. Figgis, K. Lange, D. Daßler, H. Hanifi, F. Wolfertstetter, V. Naumann, C. Hagendorf, R. Gottschalg, J. Bagdahn, Techno-economic assessment of soiling losses and mitigation strategies for solar power generation, Joule 3 (2019) 2303–2321, https://doi.org/10.1016/j.joule.2019.08.019.
[11] W. Javed, B. Guo, B. Figgis, L. Martin Pomares, B. Aïssa, Multi-year field assessment of seasonal variability of photovoltaic soiling and environmental factors in a desert environment, Solar Energy 211 (2020) 1392–1402, https://doi.org/10.1016/j.solener.2020.10.076.
[12] N. Boddupalli, G. Singh, L. Chandra, B. Bandyopadhyay, Dealing with dust – Some challenges and solutions for enabling solar energy in desert regions, Solar Energy 150 (2017) 166–176, https://doi.org/10.1016/j.solener.2017.04.032.
[13] Md.B. Yeamin, H.M. Shoaib, M.S. Hossain, A.E.M. Abdullah, S.E.M. Obaidullah, A. K.M.E. Islam, A. Rahman, Simulation and survey-based feasibility study of concentrated solar plant in northern and central Bangladesh, Results. Eng. 23 (2024) 102711, https://doi.org/10.1016/j.rineng.2024.102711.
[14] T. Sarver, A. Al-Qaraghuli, L.L. Kazmerski, A comprehensive review of the impact of dust on the use of solar energy: history, investigations, results, literature, and mitigation approaches, Renewable and Sustainable Energy Reviews 22 (2013) 698–733, https://doi.org/10.1016/j.rser.2012.12.065.
[15] P.W. Heller, The Performance of Concentrated Solar Power (CSP) systems: analysis, Measurement and assessment, Woodhead Publishing, an Imprint of Elsevier, Cambridge, MA, 2017.
[16] W.T. Xie, Y.J. Dai, R.Z. Wang, K. Sumathy, Concentrated solar energy applications using Fresnel lenses: a review, Renewable and Sustainable Energy Reviews 15 (2011) 2588–2606, https://doi.org/10.1016/j.rser.2011.03.031.
[17] A. Jaramillo-Mora, A. Rojas-Morín, S. Quezada-García, G. Jaramillo-Soto, A. Espinosa-Bautista, J.R. Gonzalez-Parra, Y. Flores-Salgado, A. Barba-Pingarrón, Development of a novel concentrated solar-powered material extrusion system for producing printed circuit assemblies, Results. Eng. 24 (2024) 103204, https://doi.org/10.1016/j.rineng.2024.103204.

[18] A. Heimsath, P. Nitz, Scattering and specular reflection of solar reflector materials – Measurements and method to determine solar weighted specular reflectance, Solar Energy Materials and Solar Cells 203 (2019) 110191, https://doi.org/10.1016/j.solmat.2019.110191.
[19] A. Fernández-García, F. Sutter, L. Martínez-Arcos, C. Sansom, F. Wolfertstetter, C. Delord, Equipment and methods for measuring reflectance of concentrating solar reflector materials, Solar Energy Materials and Solar Cells 167 (2017) 28–52, https://doi.org/10.1016/j.solmat.2017.03.036.
[20] F. Wolfertstetter, F. Sutter, E. Lüpfert, M. Montecchi, C. Heras, G. Bern, F. Ise, M. Bitterling, A. Heimsath, F. Ise, A. Fernández-García, J. Wette, A. Asselineau, I. Energy, G. Zhu, Recommendations for reflectance measurements on soiled solar mirrors (2022).
[21] M. Montecchi, Proposal of a new parameter for the comprehensive qualification of solar mirrors for CSP applications, AIP Conf Proc 1734 (2016) 130014, https://doi.org/10.1063/1.4949224.
[22] F. Sutter, M. Montecchi, H. von Dahlen, A. Fernández-García, M. Röger, The effect of incidence angle on the reflectance of solar mirrors, Solar Energy Materials and Solar Cells 176 (2018) 119–133, https://doi.org/10.1016/j.solmat.2017.11.029.
[23] A. Fernandez-Garcia, F. Sutter, M. Montecchi, F. Sallaberry, A. Heimath, C. Heras, E. Le Baron, A. Soum-Glaude, Parameters and method to evaluate the reflectance properties of reflector materials for concentrating Solar power technology technology - official reflectance guideline version 3.1, SolarPACES (2020).
[24] J. Wette, F. Sutter, R. Sánchez-Moreno, A. Fernández-García, Comparison of Commercial Reflectometers for Solar Mirrors, SolarPACES Conference Proceedings 1 (2022), https://doi.org/10.52825/solarpaces.v1i.666.
[25] C. Sansom, A. Fernández-García, P. King, F. Sutter, A. García-Segura, Reflectometer comparison for assessment of back-silvered glass solar mirrors, Solar Energy 155 (2017) 496–505, https://doi.org/10.1016/j.solener.2017.06.053.
[26] F. Wolfertstetter, K. Pottler, N. Geuder, R. Affolter, A.A. Merrouni, A. Mezrhab, R. Pitz-Paal, Monitoring of mirror and sensor soiling with TraCS for improved quality of ground based irradiance measurements, Energy Procedia 49 (2014) 2422–2432, https://doi.org/10.1016/j.egypro.2014.03.257.
[27] A. Heimsath, T. Schmidt, J. Steinmetz, C. Reetz, M. Schwandt, R. Meyer, P. Nitz, Automated monitoring of soiling with AVUS instrument for improved solar site assessment, Santiago, Chile (2018) 190008, https://doi.org/10.1063/1.5067193.
[28] Á.Fernández Solas, N. Riedel-Lyngskær, N. Hanrieder, F. Norde Santos, S. Wilbert, H. Nygard Riise, J. Polo, E.F. Fernández, F. Almonacid, D.L. Talavera, L. Micheli, Photovoltaic soiling loss in Europe: geographical distribution and cleaning recommendations, Renew Energy 239 (2025) 122086, https://doi.org/10.1016/j.renene.2024.122086.
[29] W.K. Yap, R. Galet, K.C. Yeo, Quantitative Analysis of Dust and Soiling on Solar PV Panels in the Tropics Utilizing Image-Processing Methods, (n.d.) (2025).
[30] M.Z.E. Rafique, H.M.R. Faruque, A. Hassan, M. Tian, N. Das, Y. Yao, Field deployable mirror soiling detection based on polarimetric imaging, SolarPACES Conference Proceedings 1 (2022), https://doi.org/10.52825/solarpaces.v1i.621.
[31] F. Wiesinger, S. Baghouil, E.L. Baron, R. Collignon, F. Santos, T.C. Diamantino, I. Catarino, J. Facão, C. Ferreira, S. Páscoa, F. Sutter, A. Fernández-García, J. Wette, Detection of corrosion on silvered glass reflectors via image processing, Results. Eng. 25 (2025) 103781, https://doi.org/10.1016/j.rineng.2024.103781.
[32] F. Wolfertstetter, S. Wilbert, J. Dersch, S. Dieckmann, R. Pitz-Paal, A. Ghennioui, Integration of soiling-rate measurements and cleaning strategies in yield analysis of parabolic trough plants, J Sol Energy Eng 140 (2018) 041008–041008–11, https://doi.org/10.1115/1.4039631.
[33] E. Karnezi, F. Wolfertstetter, N. Hanrieder, S. Wilbert, S. Basart, A. Soret, C. Perez Garcia-Pando, Developing soiling forecasts for optimizing operation and maintenance procedures in CSP plants, Offenbach, Germany (2019). https://elib.dlr.de/126707/(accessed. January 28, 2021).
[34] F. Sutter, A. Fernández-García, A. Heimsath, M. Montecchi, C. Pelayo, Advanced measurement techniques to characterize the near-specular reflectance of solar mirrors, AIP Conf Proc 2126 (2019) 110003, https://doi.org/10.1063/1.5117618.
[35] R. Conceição, A. Martínez Hernández, M. Romero, J. González-Aguilar, Experimental soiling assessment, characterization and modelling of a highly-compact heliostat field in an urban environment, Solar Energy 262 (2023) 111812, https://doi.org/10.1016/j.solener.2023.111812.
[36] A. Alami Merrouni, R. Conceição, A. Mouaky, H.G. Silva, A. Ghennioui, CSP performance and yield analysis including soiling measurements for Morocco and Portugal, Renew Energy 162 (2020) 1777–1792, https://doi.org/10.1016/j.renene.2020.10.014.
[37] A.A. Hachicha, I. Al-Sawafta, D.Ben Hamadou, Numerical and experimental investigations of dust effect on CSP performance under United Arab Emirates weather conditions, Renew Energy 143 (2019) 263–276, https://doi.org/10.1016/j.renene.2019.04.144.
[38] A. Azouzoute, A.A. Merrouni, M. Garoum, E.G. Bennouna, Soiling loss of solar glass and mirror samples in the region with arid climate, Energy Reports 6 (2020) 693–698, https://doi.org/10.1016/j.egyr.2019.09.051.
[39] J. Wette, A. Fernández-García, F. Sutter, F. Buendía-Martínez, D. Argüelles-Arízcun, I. Azpitarte, G. Pérez, Water saving in CSP plants by a novel hydrophilic anti-soiling coating for solar reflectors, Coatings 9 (2019) 739, https://doi.org/10.3390/coatings9110739.
[40] D. Dahlioui, J. Wette, A. Fernández-García, H. Bouzekri, I. Azpitarte, Performance assessment of the anti-soiling coating on solar mirrors soiling in the arid climate of Ouarzazate-Morocco, Solar Energy 241 (2022) 13–23, https://doi.org/10.1016/j.solener.2022.05.063.
[41] G. Picotti, R. Simonetti, T. Schmidt, M.E. Cholette, A. Heimsath, S.J. Ernst, G. Manzolini, Evaluation of reflectance measurement techniques for artificially soiled solar reflectors: experimental campaign and model assessment, Solar Energy Materials and Solar Cells 231 (2021) 111321, https://doi.org/10.1016/j.solmat.2021.111321.
[42] P. King, C. Sansom, H. Almond, M. Karim, L.R. Idiazabal, Simulation of the Effect of Dust Barriers On the Reduction of Mirror Soiling in CSP Plants, AIP Publishing LLC, 2020 210004.
[43] F. Wolfertstetter, Effects of Soiling on Concentrating Solar Power Plants, Hochschulbibliothek der Rheinisch-Westfälischen Technischen Hochschule Aachen, 2016. Ph.D. thesis.
[44] F. Wolfertstetter, S. Wilbert, F. Terhag, N. Hanrieder, A. Fernandez-García, C. Sansom, P. King, L. Zarzalejo, A. Ghennioui, Modelling the soiling rate: dependencies on meteorological parameters, AIP Conf Proc 2126 (2019) 190018, https://doi.org/10.1063/1.5117715.
[45] L. Micheli, M. Muller, An investigation of the key parameters for predicting PV soiling losses, Progress in Photovoltaics: Research and Applications 25 (2017) 291–307, https://doi.org/10.1002/pip.2860.
[46] R. Conceição, H.G. Silva, M. Collares-Pereira, CSP mirror soiling characterization and modeling, Solar Energy Materials and Solar Cells 185 (2018) 233–239, https://doi.org/10.1016/j.solmat.2018.05.035.
[47] A. Pfahl, J. Coventry, M. Röger, F. Wolfertstetter, J.F. Vásquez-Arango, F. Gross, M. Arjomandi, P. Schwarzbözl, M. Geiger, P. Liedke, Progress in heliostat development, Solar Energy 152 (2017) 3–37, https://doi.org/10.1016/j.solener.2017.03.029.
[48] G.J. Kolb, Heliostat Cost Reduction Study, Sandia, Albuquerque, USA, 2007.
[49] J.B. Blackmon, M. Douglas, Non-Inverting Hellostat Study - Effects Of Dust Buildup, Sandia, 1979.
[50] J.B. Blackmon, Non-Inverting Heliostat Study, Sandia, 1979.
[51] A. Kerstein, Evaluation of inverted-stow capability for heliostats, 1981. https://doi.org/10.2172/6150925.
[52] G. Zhu, J. Sment, C. Turchi, M. Gordon, R. Brost, R. Mitchell, D. Kesseli, T. Farrell, M. Muller, K. Armijo, M. Cholette, M. Emes, A. Zolan, C. Augustine, S. Meyen, D. Tsvankin, S. Yellapantula, P. Kurup, W. Hamilton, D. Small, A. Spieles, M. Collins, J. Coventry, K. Kattke, M. Izygon, R. Sommers, E. Tsiropoulou, Heliostat Consortium Annual Report: 2024, US Department of Energy (2024).
[53] G. Zhu, C. Augustine, R. Mitchell, M. Muller, P. Kurup, A. Zolan, S. Yellapantula, R. Brost, K. Armijo, J. Sment, R. Schaller, M. Gordon, M. Collins, J. Coventry, J. Pye, M. Cholette, G. Picotti, M. Arjomandi, M. Emes, D. Potter, M. Rae, Roadmap to advance Heliostat technologies for concentrating solar-thermal power, 2022. https://doi.org/10.2172/1888029.
[54] F. Sutter, S. Meyen, A. Fernández-García, P. Heller, Spectral characterization of specular reflectance of solar mirrors, Solar Energy Materials and Solar Cells 145 (2016) 248–254, https://doi.org/10.1016/j.solmat.2015.10.030.
[55] IEC, 60904-3:2019. Photovoltaic devices – Part 3: measurement principles for terrestrial photovoltaic (PV) solar devices with reference spectral irradiance data. https://webstore.iec.ch/en/publication/61084, 2019 (accessed March 6, 2025).
[56] A.M. Bonanos, A.C. Montenon, M.J. Blanco, Estimation of mean field reflectance in CST applications, Solar Energy 208 (2020) 1031–1038, https://doi.org/10.1016/j.solener.2020.08.073.
[57] Evaluation of measurement data — Guide to the expression of uncertainty in measurement, (2008).
[58] Evaluation of measurement data — Supplement 1 to the "Guide to the expression of uncertainty in measurement" — Propagation of distributions using a Monte Carlo method, (2008). https://doi.org/10.59161/JCGM101-2008.
[59] M.J. Tuman, M.J. Wagner, Neural-network-driven dynamic simulation of parabolic trough solar fields for improved CSP plant operation, Solar Energy 287 (2025) 113203, https://doi.org/10.1016/j.solener.2024.113203.
[60] E. Casati, F. Casella, P. Colonna, Design of CSP plants with optimally operated thermal storage, Solar Energy 116 (2015) 371–387, https://doi.org/10.1016/j.solener.2015.03.048.
[61] R. Kabra, Reliability availability and maintainability study for concentrated solar plants and how to account for current limitations and challenges, in: 2023 Middle East and North Africa Solar Conference, MENA-SC, 2023, pp. 1–3, https://doi.org/10.1109/MENA-SC54044.2023.10374501.
[62] F. Buendía-Martinez, A. Fernandez-Garcia, F. Sutter, L. Martinez-Arcos, T.J. Reche-Navarro, A. Garcia-Segura, L. Valenzuela, Uncertainty study of reflectance measurements for concentrating solar reflectors, IEEe Trans. Instrum. Meas. 69 (2020) 7218–7232, https://doi.org/10.1109/TIM.2020.2975387.
[63] R. Conceição, I. Vázquez, L. Fialho, D. García, Soiling and rainfall effect on PV technology in rural Southern Europe, renewable Energy 156 (2020) 743–747. https://doi.org/10.1016/j.renene.2020.04.119.
[64] C.B. Anderson, G. Picotti, T. Schmidt, M.E. Cholette, G. Bern, T.A. Steinberg, G. Manzolini, The impact of condensation on solar collector soiling: an experimental study, Solar Energy Materials and Solar Cells 275 (2024) 112998, https://doi.org/10.1016/j.solmat.2024.112998.
[65] D. Olivares, A. Marzo, A. Taquichiri, R. Espinoza, M. Henriquez, C. Portillo, P. Ferrada, L.A. Conde, E. Fuentealba, V. del Campo, Impact of thermoelectric coal-fired power plant emissions on the soiling mechanisms of nearby photovoltaic power plants in the Atacama Desert, Renew Energy 244 (2025) 122684, https://doi.org/10.1016/j.renene.2025.122684.
[66] A. Heimsath, P. Lindner, E. Klimm, T. Schmid, K.O. Moreno, Y. Elon, M. Am-Shallem, P. Nitz, Specular reflectance of soiled glass mirrors – Study on the impact of incidence angles, Cape Town, South Africa (2016) 130009, https://doi.org/10.1063/1.4949219.